UNCLASSIFIED

AD NUMBER
AD383260
CLASSIFICATION CHANGES
TO: unclassified
FROM: confidential
LIMITATION CHANGES
TO: Approved for public release, distribution unlimited
FROM: No foreign distribution.
AUTHORITY
1979 per Group-4 document markings; AFRPL ltr., 5 Feb 1986

THIS PAGE IS UNCLASSIFIED

CONFIDENTIAL

AFRPL-TR-67-226

AD 383260

(15)

(Unclassified Title)

ADVANCED THRUST CHAMBER FOR SPACE MANEUVERING PROPULSION

Tasks II and III - Thrust Chamber Segment Evaluations
Final Report - Materials and Processes

H. G. Diem
R. P. Pauckert

Rocketdyne
A Division of North American Aviation, Inc.
Canoga Park, California

TECHNICAL REPORT AFRPL-TR-67-226

July 1967

Group 4
Downgraded at 3-Year Intervals
Declassified After 12 Years

THIS MATERIAL CONTAINS INFORMATION AFFECTING THE NATIONAL DEFENSE OF THE UNITED STATES WITHIN THE MEANING OF THE ESPIONAGE LAWS, TITLE 18 U.S.C., SECTIONS 793 AND 794, THE TRANSMISSION OR REVELATION OF WHICH IN ANY MANNER TO AN UNAUTHORIZED PERSON IS PROHIBITED BY LAW.

In addition to security requirements which must be met, this document is subject to special export controls and each transmittal to foreign governments or foreign nationals may be made only with prior approval of AFRPL, Edwards, California 93523.

Air Force Rocket Propulsion Laboratory
Research and Technology Division
Edwards Air Force Base, California
Air Force Systems Command
United States Air Force

CONFIDENTIAL

CONFIDENTIAL

AFRPL-TR-67-226

(Unclassified Title)

ADVANCED THRUST CHAMBER FOR SPACE MANEUVERING PROPULSION

Tasks II and III - Thrust Chamber Segment Evaluations - Materials and Processes

H. Diem
R. P. Pauckert

Rocketdyne, a Division of North American Aviation, Inc.
6633 Canoga Avenue, Canoga Park, California

July 1967

Group 4
Downgraded at 3-Year Intervals
Declassified After 12 Years

Air Force Rocket Propulsion Laboratory
Research and Technology Division
Edwards Air Force Base, California
Air Force Systems Command
United States Air Force

CONFIDENTIAL

FOREWORD

(U) This technical report describes the materials and processes utilized under Tasks II and III of the "Advanced Thrust Chamber for Space Propulsion" program. These tasks were conducted during the period from 16 May 1966 to 30 June 1967. Additional program results were presented in reports AFRPL-TR-66-301 and AFRPL-TR-67-214. The program was authorized by the USAF Rocket Propulsion Laboratory under Contract AF04(611)-11617. The Air Force Program Manager was Mr. W. W. Wells, RPREC.

(U) This report was prepared by Rocketdyne, a Division of North American Aviation, Inc., as Report R-6730-2

(U) This report has been reviewed and is approved.

W. W. Wells, AFRPL Program Manager

ABSTRACT

(U) Materials and processes developed and used to fabricate segments of a toroidal aerospike thrust chamber are presented. A brief design description is given of solid-wall and tube-wall hot-firing segments and of nonfiring structural test segments using rib and honeycomb material for strength and rigidity. The materials used include OFHC copper, nickel 200, CRES 347, and Inconel 718. The processes described include electrodeposition, electro-discharge machining, brazing, and welding.

CONTENTS

Section I 1
Introduction and Summary 1
Section II 3
Segment Description 3
  1. General 3
  2. Solid-Wall Segments 3
  3. Tube-Wall Throat Inserts 9
  4. Tube-Wall Segments 14
  5. Structural Segments 14
Section III 23
Materials of Construction 23
  1. OFHC Copper 23
  2. Nickel 200 23
  3. CRES 347 24
  4. Inconel 718 25
  5. Braze Materials 25
Section IV 27
Fabrication Processes 27
  1. Electroplating 27
  2. Electroforming 28
  3. Electrodischarge Machining 44
  4. Brazing 47
  5. Welding 50
  6. Heat Treating 65
Section V 67
Conclusions and Recommendations 67

ILLUSTRATIONS

1. Test Hardware Interchangeability 4
2. Solid-Wall Segment Contours 6
3. Exploded View of Solid-Wall Segment 7
4. Parallel-Wall Chamber and Nozzle Cross Section (Contour C) . . 8
5. Tube-Wall Insert and Water-Cooled Chamber 10
6. Regenerative Nozzle Wafer 11
7. Tube-Wall Throat Insert Components 12
8. Nickel Tube-Wall Throat Insert 13
9. Tube-Wall Segment 15
10. Tube-Wall Segment 16
11. Structural Test Segment--Rib Supports 19
12. Composite Ribe/Honeycomb Structural Segment 21
13. Honeycomb Edge Plating Sample 29
14. Honeycomb Panels and Masks Prior to Nickel Plating 30
15. Plated Honeycomb Cores & Closeouts in Formblock 31
16. Comparison of Plated and Conventional Tubes 32
17. Location of Metallographic Specimens Removed From Electroformed Copper-347 CRES Tube 34
18. Typical Cross Section of 347 CRES Tube With Electroformed Copper Sheath on OD 35
19. Typical Microstructure of "As-Deposited" Electroformed Copper Sheath 35
20. Typical Interface (Arrows) between Copper A and 347 CRES B in "As-Deposited" Condition 36
21. Typical Radial Cracks Observed in As-Deposited Copper Sheath 36
22. OD Surface of Copper Sheath 37
23. Typical Cross Section Through Tube Section with Copper Sheath After Exposure to Hydrogen Embrittlement Test 37
24. High Magnification Photomicrograph of Section Showing Gassing (Spherical Voids) 38
25. Typical Longitudinal Section 38
26. Significant Features on Brazed Tube Sample 40
27. Brazed Copper-Plated CRES Tubes 41
28. Schematic of Bimetallic Test Section 42
29. Cross Section of Nickel-Plated Tube (200X) 43
30. Tube Bank Showing Nonconcentric Tubes 45
31. Joint Between Tube Bundle and Manifold 46
32. Required Fillet Size vs Alloy Strength 49
33. Face Sheet to Honeycomb Braze 51
34. Sample EB-Welded Tube Blankets Before and After Forming . . 52
35. Microphoto of Electron-Beam Welded Nickel Tubes 54
36. Electron Beam Welded CRES 347 Tubes 55
37. Partial Assembly of Rib Panel 56

38. Rib Weld Sample 58
39. Final Weld Configurations Selected for Welding
Channel Ends to Rib Section Closeouts 59
40. Rib Panel Before Welding 60
41. Rib Panel After EB Welding 61
42. Nickel Plating and Weld Sample 63
43. Plated Edge Joint Weld Sample 64
44. Typical Channel to Channel Rib Panel Weld 66

TABLES

1. Thrust Chamber Contour Characteristics 5
2. Comparison of Nickel 200, OFHC Copper, and CRES 347 24
3. Braze Alloys Used in Segment Fabrication 26

SECTION I

INTRODUCTION AND SUMMARY

(U) As a result of efforts under Contract AF04(611)10745, the present study was undertaken to experimentally and analytically evaluate the critical design aspects of the toroidal combustion chamber for an aerospike engine. The primary parameters investigated were performance (c* efficiency), regenerative cooling capability, and structural integrity.

(U) The first two objectives were achieved by fabricating and firing water-cooled and tube-wall, hydrogen-cooled segments of the complete toroidal chamber. Structural integrity and rigidity were demonstrated in segments of lightweight design using ribs and honeycomb as the structural material. The structural segments were not hot fired but were subjected to hydraulic pressure to simulate the effect of chamber pressure.

(U) Because of the similarity of components, the major materials used were few in number. OFHC copper and nickel 200 were used in the hot-firing segments because of their good thermal conductivity characteristics. CRES 347 was also used because of its high strength at elevated temperatures. Inconel 718 was used in the structural segments because of its low coefficient of thermal expansion and high strength.

(C) Several processes of interest were employed or developed during the course of this effort. Those processes which required development of critical techniques or selection of materials were investigated economically on as basic a level as practical. Electroplating was used to protect the nozzle throat surface of the water-cooled copper segments and to prepare components for brazing. Electroforming operations were evolved to produce two types of hydrogen coolant tubes for the combustion chamber, which had a constant outside diameter and a variable inside diameter. The two types were copper deposited on CRES tubes and nickel on nickel tubes. The nickel on nickel electroformed tubes resulted in nonconcentric cross sections. Electroforming was also used to increase the thickness of the edges of honeycomb sections. These nickel-electroformed edges were required for welding the honeycomb pieces to thicker components.

(U) Electrodischarge machining processes were used to form the contours of the nozzle throat sections and, in some instances, the combustion chamber sections of the solid-wall hot-firing segments. This process was also investigated as a means of obtaining very small holes in the walls of coolant tubes with a small angle between the axes of the hole and the tube. Smaller holes and angles were obtainable with the electrodischarge technique than with conventional mechanical drilling methods.

(U) Brazing processes were used extensively in assembly the segments. The coolant tubes used were, in all cases, brazed to the copper support structure which resisted chamber pressure loads. One solid-wall segment combustion chamber, both tube-wall throat inserts, and both tube-wall segments were assembled by brazing all or some of the component parts together. The panels for the honeycomb structural segment were produced by brazing sheets of Inconel to the honeycomb core pieces with a high strength alloy, Palniro 7.

(C) All welding was done using the electron beam process. This process was applied to preparation of panels of cooling tubes where the tubes were welded into flat panels before being bent to form the contour of the combustion chamber wall. Good tube-to-tube welds were obtained in CRES tubes with 0.010 inch walls and nickel tubes with 0.010 to 0.024 inch walls. The process was an improvement over the previous technique of forming each tube individually and brazing the tubes together. The structural segments were assembled by electron beam welding the major components (injectors, baffles, panels, and sideplates) together. In addition, the panels for the rib structural segment were formed by electron beam welding U shaped channels together.

SECTION II

SEGMENT DESCRIPTION

1. GENERAL

(C) The items fabricated and tested during this program were segments of the toroidal combustion chamber of an aerospike engine. The engine used LF_2/LH_2 propellants at a mixture ratio of 13:1 (O/F) and chamber pressure of 650 psia to produce 30,000 pounds of thrust under vacuum conditions. Four types of segments were fabricated: (1) solid-wall hot-firing segments with water cooling of the complete item; (2) tube-wall throat inserts which had one wall cooled by a bank of tubes through which hydrogen coolant flowed (the remaining walls were water-cooled); (3) tube-wall segments with both walls covered with hydrogen-cooled tubes (water-cooled side walls) and (4) structural test segments of near-flightweight design which were not fired but were subjected to mechanical loading tests. The first three items did not require lightweight construction.

(U) The hot firing combustion chambers, nozzles and injectors were designed to represent a 3.0-inch segment of the complete toroidal chamber. Since the curvature effect over this small increment was not significant the segments were two-dimensional, i.e., the injector faces and throats were plane surfaces.

(U) The hardware was designed for maximum interchangeability between solid-wall chambers, injectors, and the subsequently fabricated tube-wall inserts and tube-wall segments. This interchangeability is illustrated in Fig. 1. The injectors were designed to fit both the solid-wall and the tube-wall segments. The solid-wall segments consisted of a combustion chamber section and a nozzle section. This sectioning permitted various combustion chamber contours to be tested with the same injector and nozzle pieces and, later, allowed the optimum chamber/injector combination to be tested with the tube-wall throat inserts.

(U) The structural test segments were independent of the hot-firing segments. Rib and honeycomb structural members were designed. A complete rib segment was fabricated which included a removable outer wall similar to a flight design engine. An outer wall only was fabricated with honeycomb and bolted to the rib inner wall for structural test.

2. SOLID-WALL SEGMENTS

(C) The purpose of these segments was to investigate the influence of injector configuration and chamber shape on performance and heat transfer characteristics. Therefore, a number of injector and chamber contour configurations were fabricated. The fabrication of the combustion chambers was particularly significant from a materials and

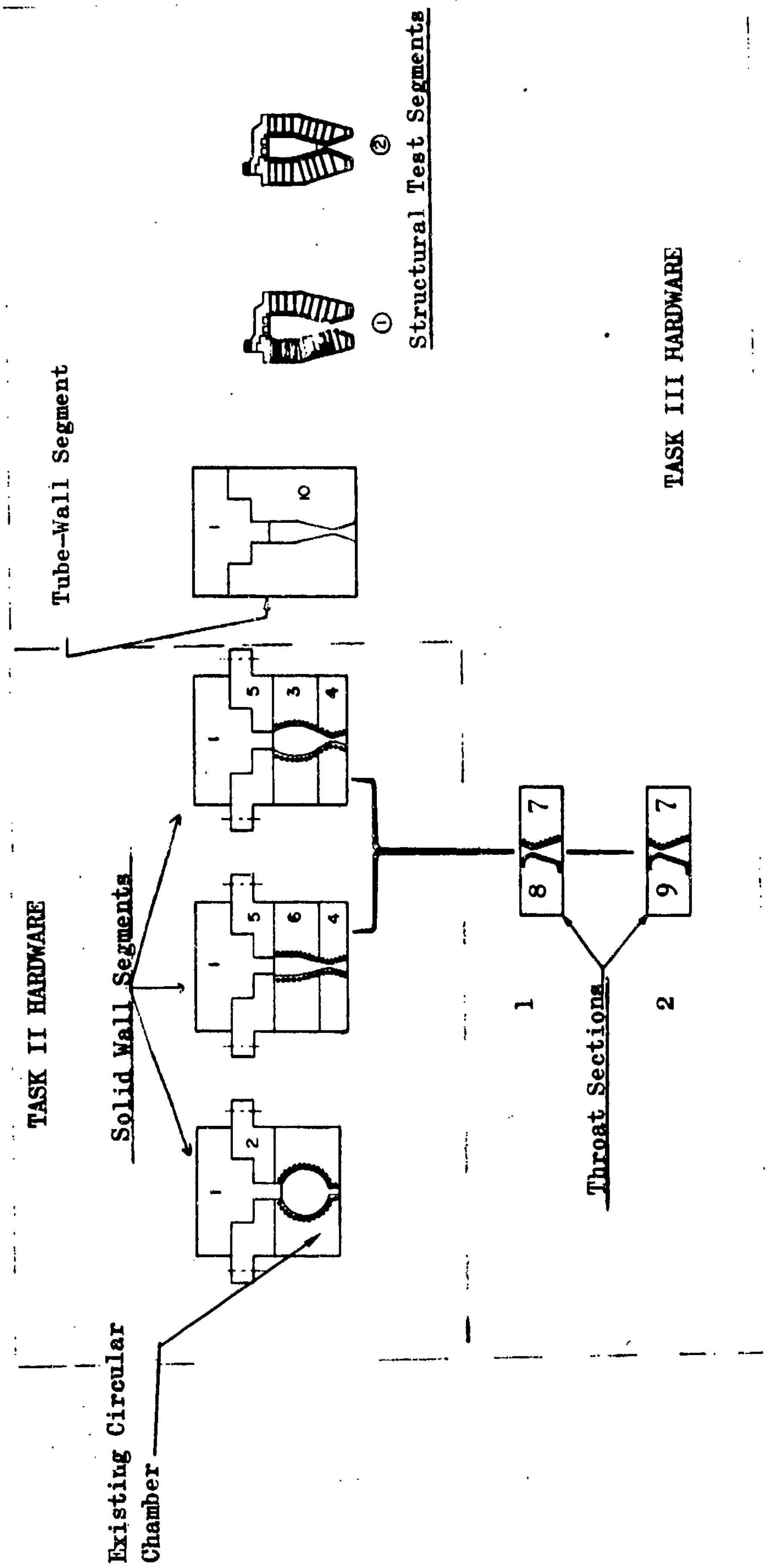

Figure 1. . Test Hardware Interchangeability

(C) processes standpoint. The shapes of the contoured walls of these chambers are shown in Fig. 2. The distance from the injector to the throat was 3.5 inches for all contours except contour D which was 1.5 inches longer. Other pertinent data for the contours are presented in Table 1. The other two walls (the walls in the plane of the paper) were plane surfaces for all contours. The throat gap dimension was 0.167 inches and the injector width was 1.0 inches for all cases. Another contour was designed under Company sponsorship and had a 2-inch injector width and continuous convergence to the throat.

TABLE 1

THRUST CHAMBER CONTOUR CHARACTERISTICS

Contour	Injector-Throat Distance, inches	Nominal Convergence Angle, degrees	Maximum Contraction Area Ratio	Expansion Nozzle Area Ratio	Contour Wall Shape
A	3.5	60	18		Circular
B	3.5	30	12	4	Curved
C	3.5	30	7	4	Straight
D	5.0	15	7	5.45	Straight
E	3.5	15	7	5.45	Straight

(U) These solid wall segments were fabricated in sections (from one to four depending upon the contour) for flexibility and ease of fabrication. In contour E, for example, the machining of the contour walls was simplified considerably by sectioning at the start of the converging region. Addition of another identical parallel-wall section converted contour E to contour D. The sections were bolted to each other and to the injector and adapter. Figure 3 is a photograph of the sections of a solid-wall segment including the facility mounting sections. Contours A, B, and C were made by brazing together the premachined side and contour walls, as described later, for the tube-wall throat inserts. All other sections were made from solid OFHC copper billets.

(U) All combustion chamber and nozzle sections were water cooled to permit extended duration tests and to provide local heat transfer data along the contour. Individual water coolant passages were provided as shown in Fig. 4. For each passage, coolant water entered the segment and was divided along two paths: one portion cooled one side wall and contour wall in series; the other portion cooled the opposite side wall and contour wall. The two flows then converged and exited through a common outlet.

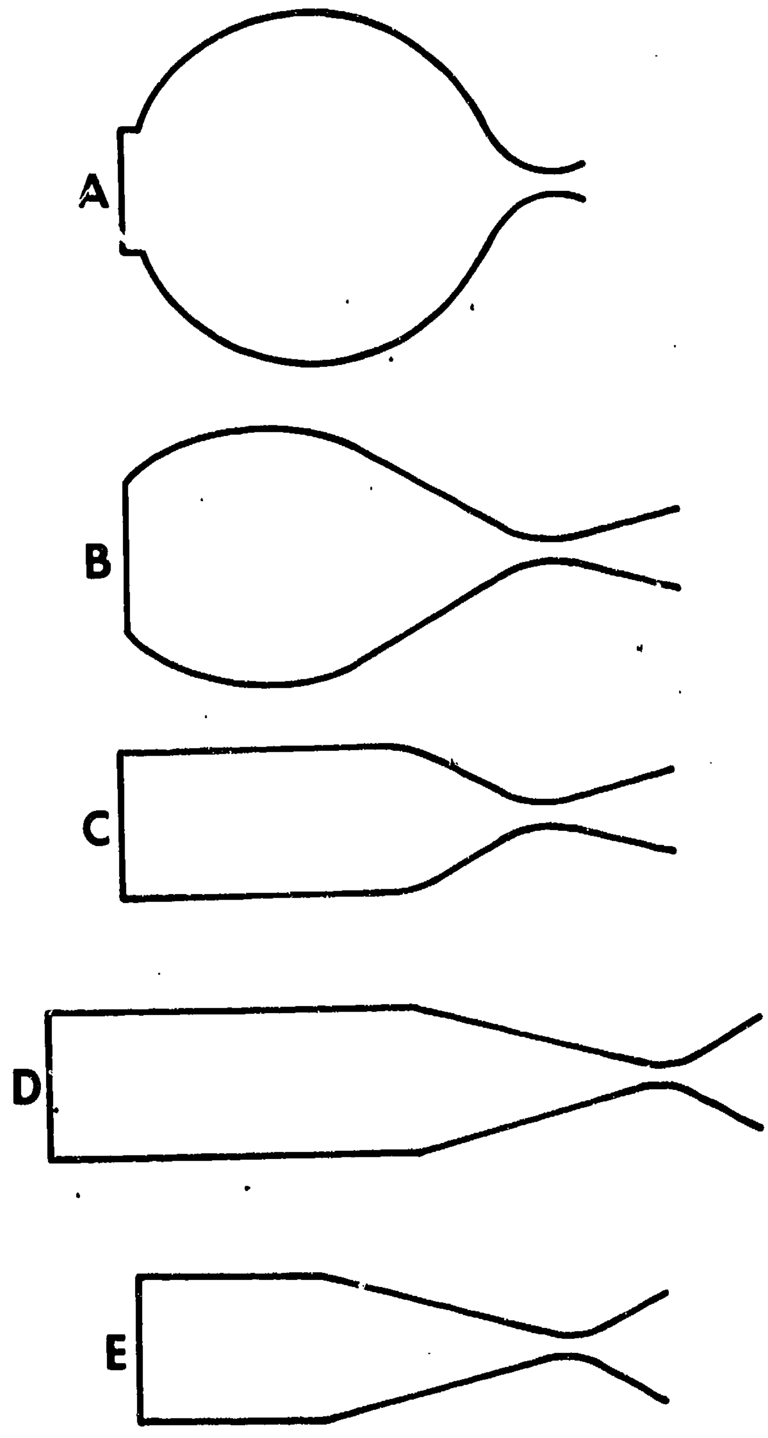

Figure 2 . Solid-Wall Segment Contours

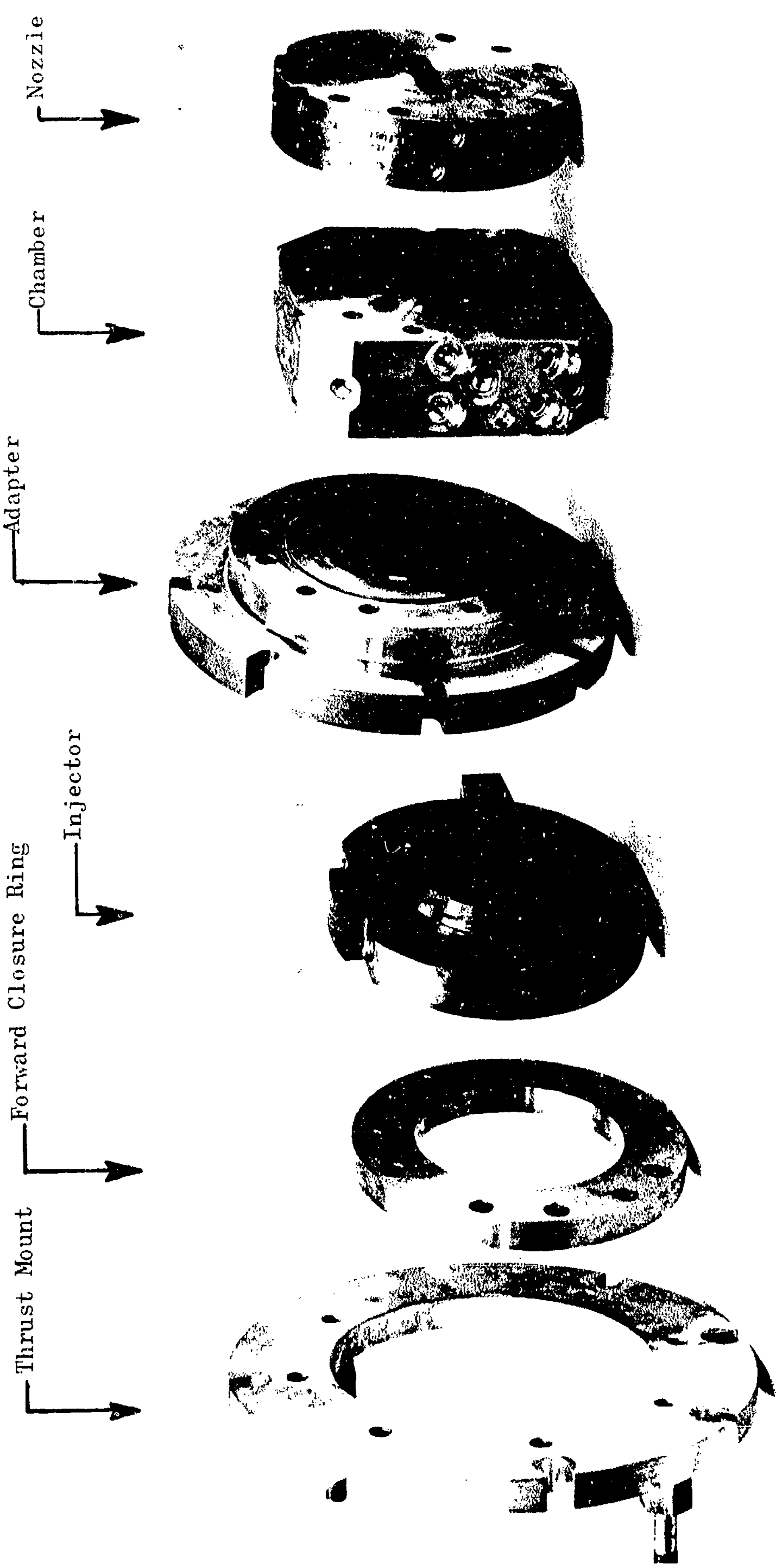

Figure 3. Exploded View of Solid-Wall Segment

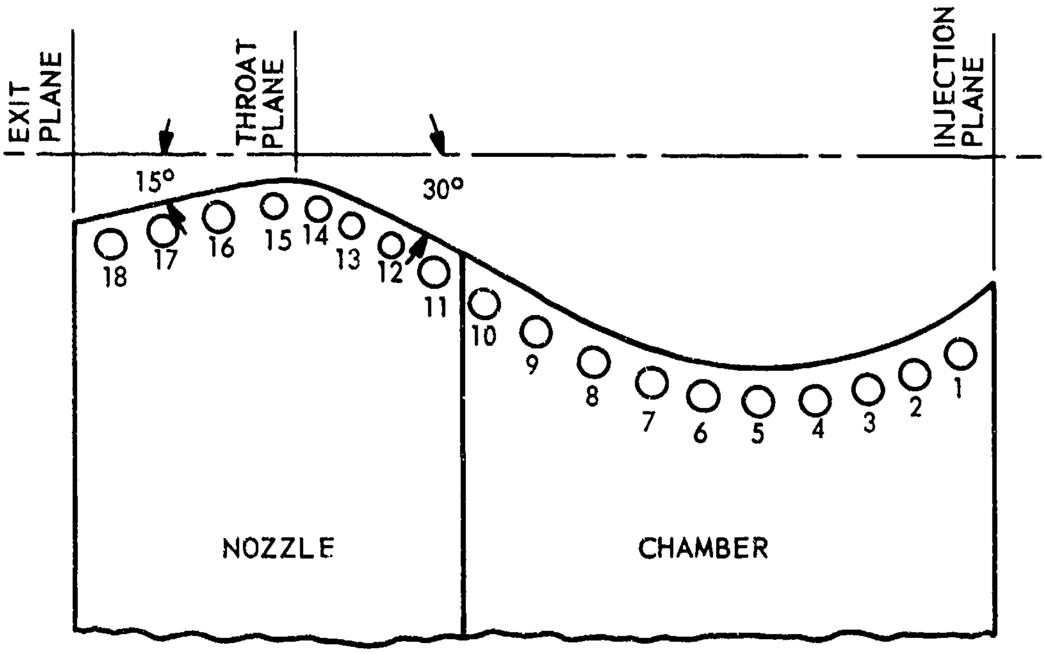

30-Degree Chamber and Nozzle Cross Section (Contour B)

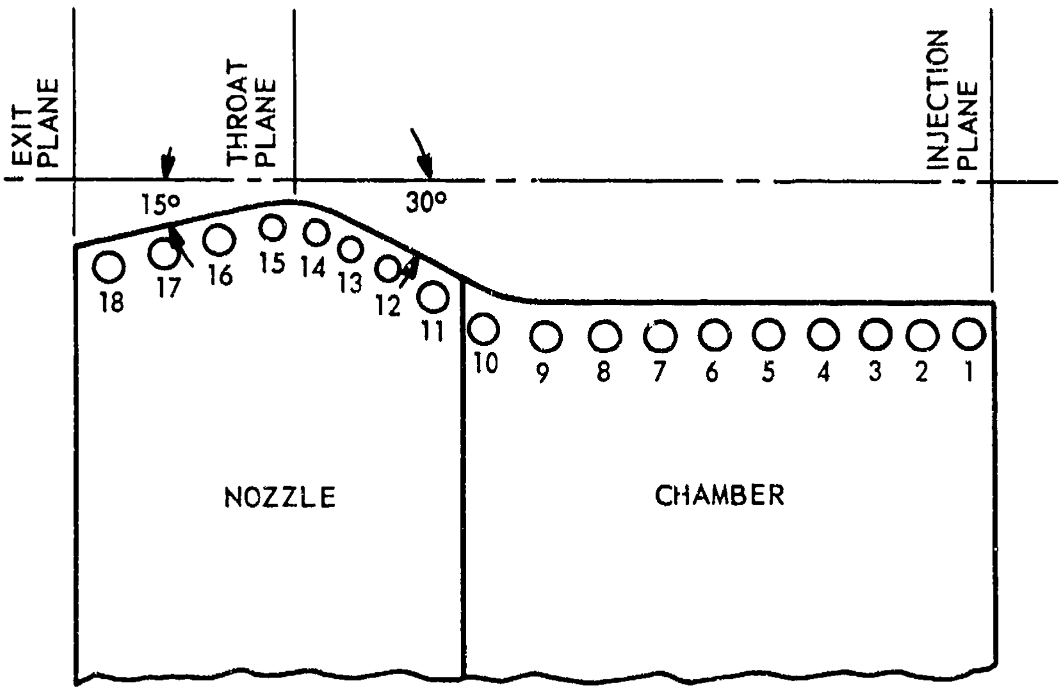

Figure 4. Parallel-Wall Chamber and Nozzle Cross Section (Contour C)

3. TUBE-WALL THROAT INSERTS

(U) Hardware for tube-wall throat section evaluation testing was assembled by using injectors, injector adapters, and combustion chamber sections from the solid-wall segments. To these components, a tube-wall throat test section was attached (Fig. 5). The tube-wall throat test section was similar to the all-water-cooled throat section, with the exception that one-half of the double expansion contour was replaced by a separate block of material assembled with longitudinally oriented, constant-diameter tubes defining the proper contour and simulating the prototype, regenerative-cooling circuit. The other contour wall and side walls were of solid-wall construction with water-coolant passages entering through the side of the wafer. From the side of the wafer, the water-cooled passages ran parallel to the side wall, across the nozzle, parallel to the opposite side wall, and out the opposite side of the throat wafer. Each of the eight passages was a separate circuit to isolate different heat fluxes within the throat section.

(U) The regenerative tubes on the nozzle contour wall were hydrogen cooled. They were located over a support body and brazed in place. Each end of the tubes was fed from separate manifolds which ran out the side of the wafer section. Pressure and temperature instrumentation ports were provided in each manifold. Coolant within the throat tubes could be flowed in either direction. A cross section of the tube-wall insert is shown in Fig. 6.

(C) Two throat insert configurations were designed and fabricated using tubes of different materials and sizes as follows:

Nickel	0.093 OD by 0.024 wall (32 required)
Stainless Steel	0.062 OD by 0.012 wall (48 required)

(U) Unlike the solid-wall throat section, the tube-wall throat insert was fabricated from several pieces. The two major pieces were the collar and core. The collar was a one-piece copper ring which served as a structural member. The core was assembled into the collar so that the water, hydrogen, and instrumentation passages passed from the core through the collar. The core itself consisted of the elements shown in Fig. 7. The tube-wall side is shown after the tubes had been formed and brazed to the support member. The two pieces on either side of the tube-wall side are the face plates, most of which are machined off after brazing. The two water-cooled side walls are shown in the center of the photograph. The water coolant holes which match the hole pattern in the water-cooled contour wall shown on the right are visible. The completed tube-wall throat insert is shown in Fig. 8. The large tubes are for the hydrogen coolant, the small tubes conduct the coolant water in and out. The core/collar interface is visible in this photograph.

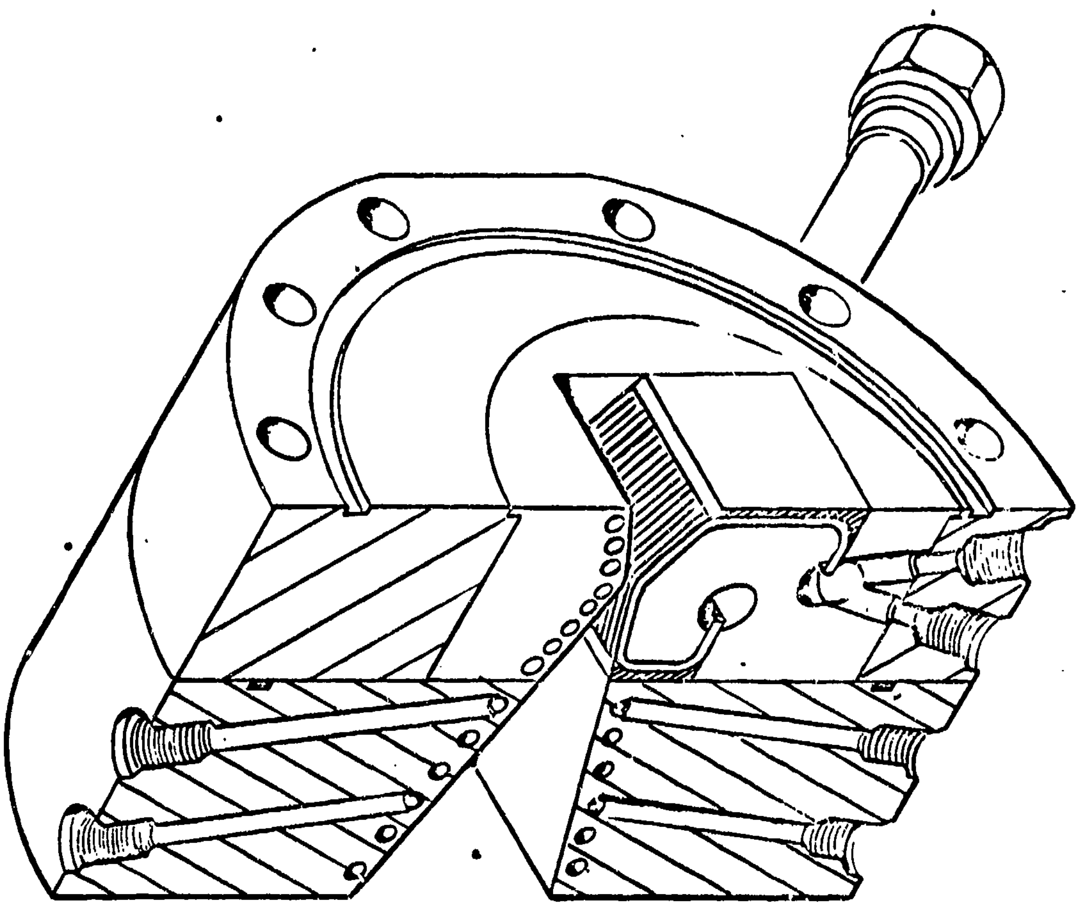

Figure 5. Tube-Wall Insert and Water-Cooled Chamber

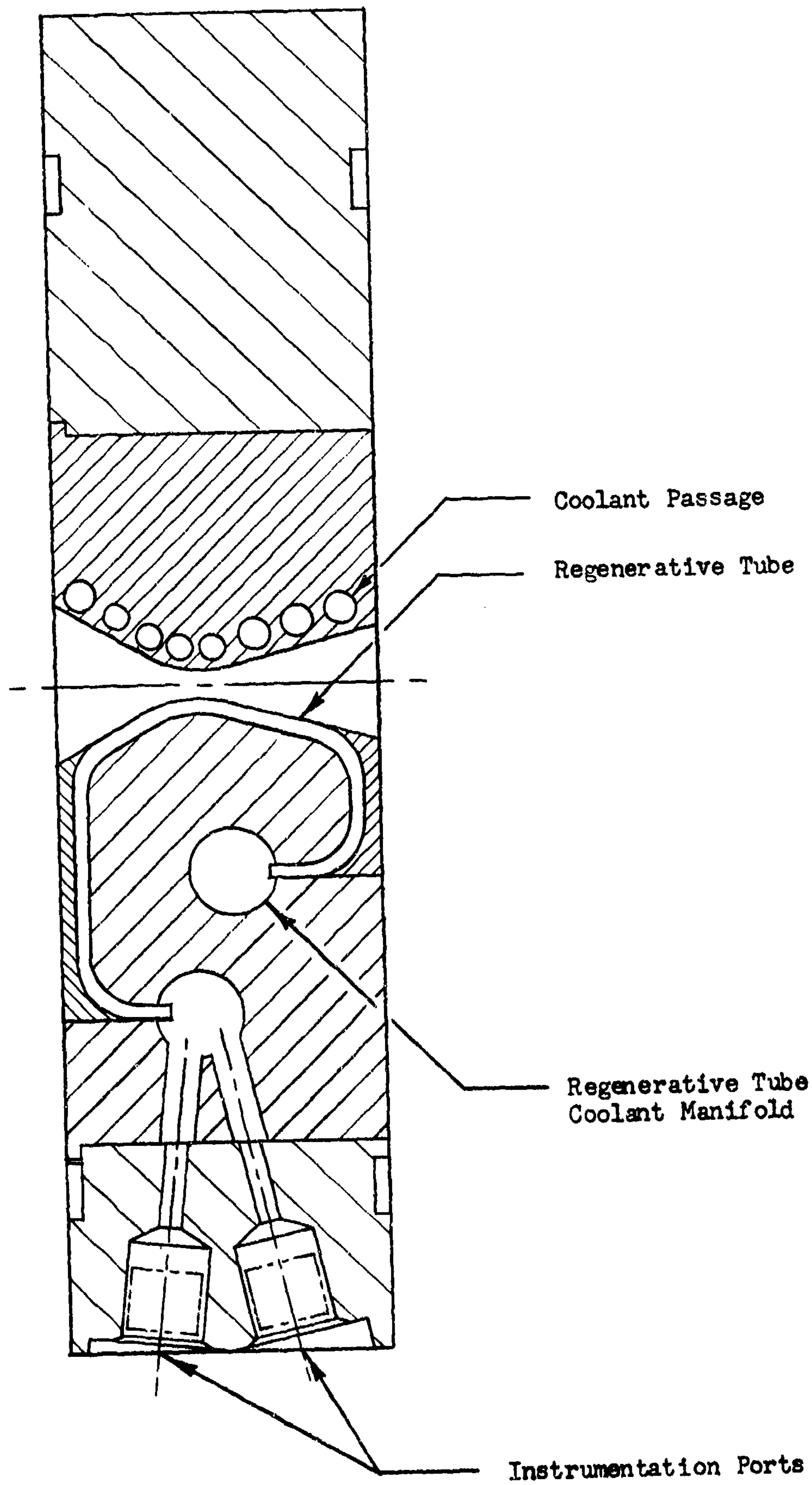

Figure 6. Regenerative Nozzle Wafer

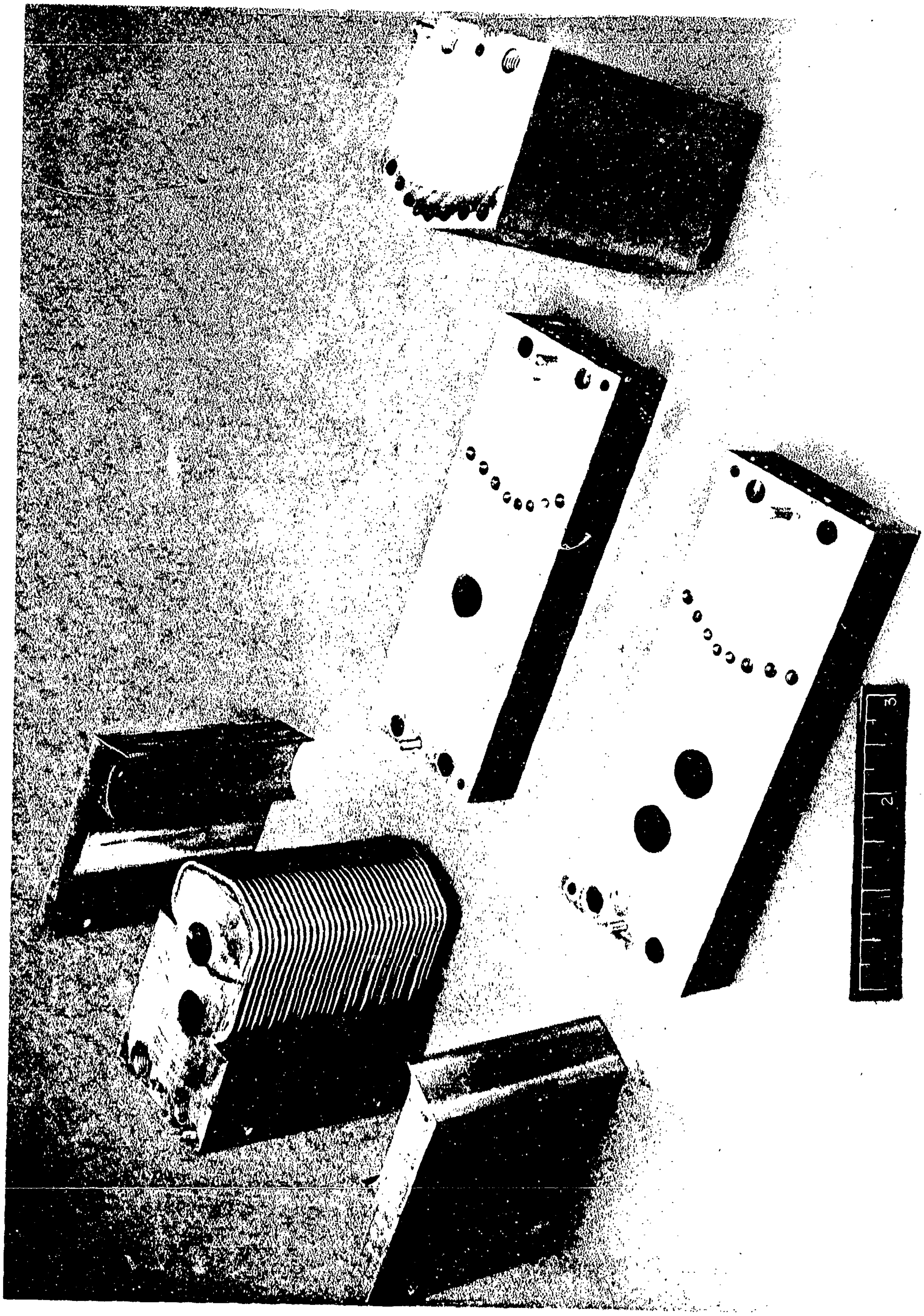

Figure 7 . Tube-Wall Throat Insert Components

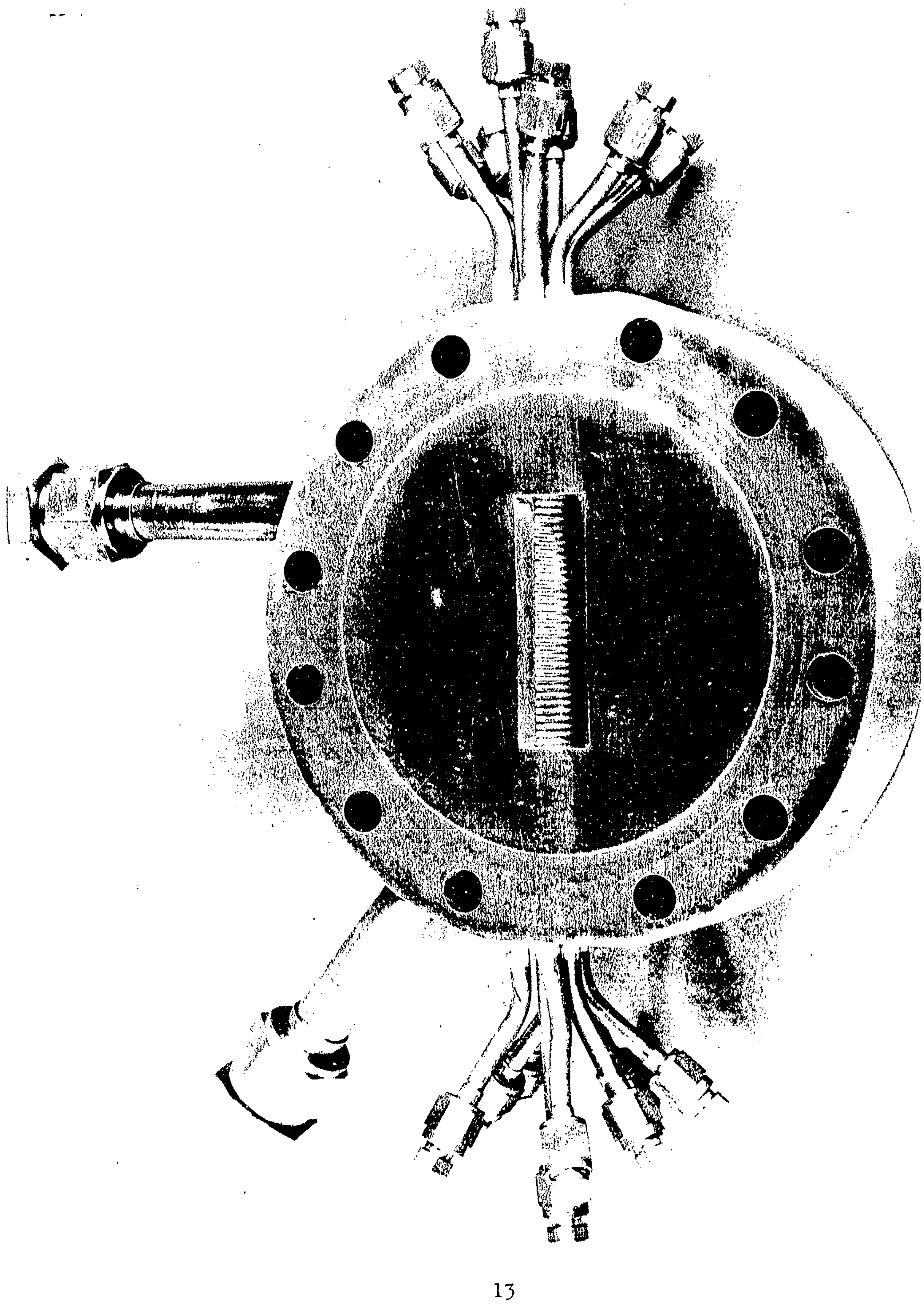

Figure 8 . Nickel Tube-Wall Throat Insert

4. TUBE-WALL SEGMENTS

(C) The purpose of the tube-wall segment was to demonstrate complete regenerative cooling capability for the thrust chamber. An isometric view of the assembly is shown in Fig. 9. The segment was provided with two-pass hydrogen cooling of each contour wall. After cooling one side of the segment, the hydrogen could be externally ducted to the opposite contour wall. After cooling the second wall, the hydrogen was either dumped or conducted into the injector manifold. The segment was designed to accept the 2-inch wide injector used with the solid-wall segments. The tube walls converged at a continuous 17-degree angle to the throat then diverged at a 15-degree angle to an area ratio of 4 at the nozzle exit.

(U) The core-and-collar construction was used. In this case, the collar was made of 347 CRES. The assembly details are seen more clearly in the exploded view of the segment shown in Fig. 10. The core was formed by the strongbacks, which support the contoured tube bundles, and the side walls (side plates). The side walls of the segment were water-cooled. Each side wall had individual inlet and outlet water manifolds which were connected by drilled passages. The length and diameter of these passages were varied to ensure proper distribution of flow along the length of the chamber.

5. STRUCTURAL SEGMENTS

(C) The purpose of these segments was to demonstrate structural integrity and rigidity of lightweight structures under mechanical loading conditions which would simulate chamber pressure loads. The segments tested demonstrated throat gap (area) variations of less than 3 percent under chamber pressure variations of 0 to 650 psig. The combustion chamber of the flight design engine consisted of inner and outer walls connected by the injector and by 24 equally spaced subsonic baffles. The outer wall was removable and was bolted to the injector and to the baffle. Three bolts were used to fasten the outer wall at each baffle.

(U) Hydraulic pressure was used in the structural segment testing to simulate chamber pressure. The side plates used to contain the pressure in the segment introduced end effects, so a three-compartment (two baffles) segment was designed so that data taken on the center compartment would not be significantly influenced by these end effects. The segments were approximately 21 inches long. Two segments were designed: one used rib members to provide rigidity to resist deflections resulting in throat gap variations; the other segment used honeycomb for rigidity. The honeycomb wall was fabricated by brazing face sheets to both sides of a honeycomb core. Analysis revealed that valid data could be obtained for both types of structure by testing a complete rib segment and a composite segment using the rib segment inner wall and a honeycomb outer wall.

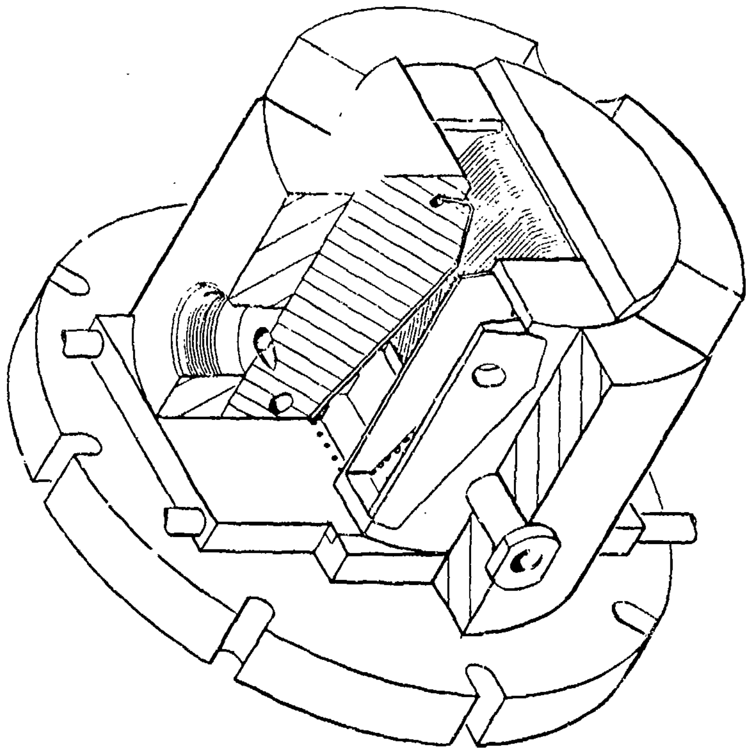

Figure 9. Tube-Wall Segment

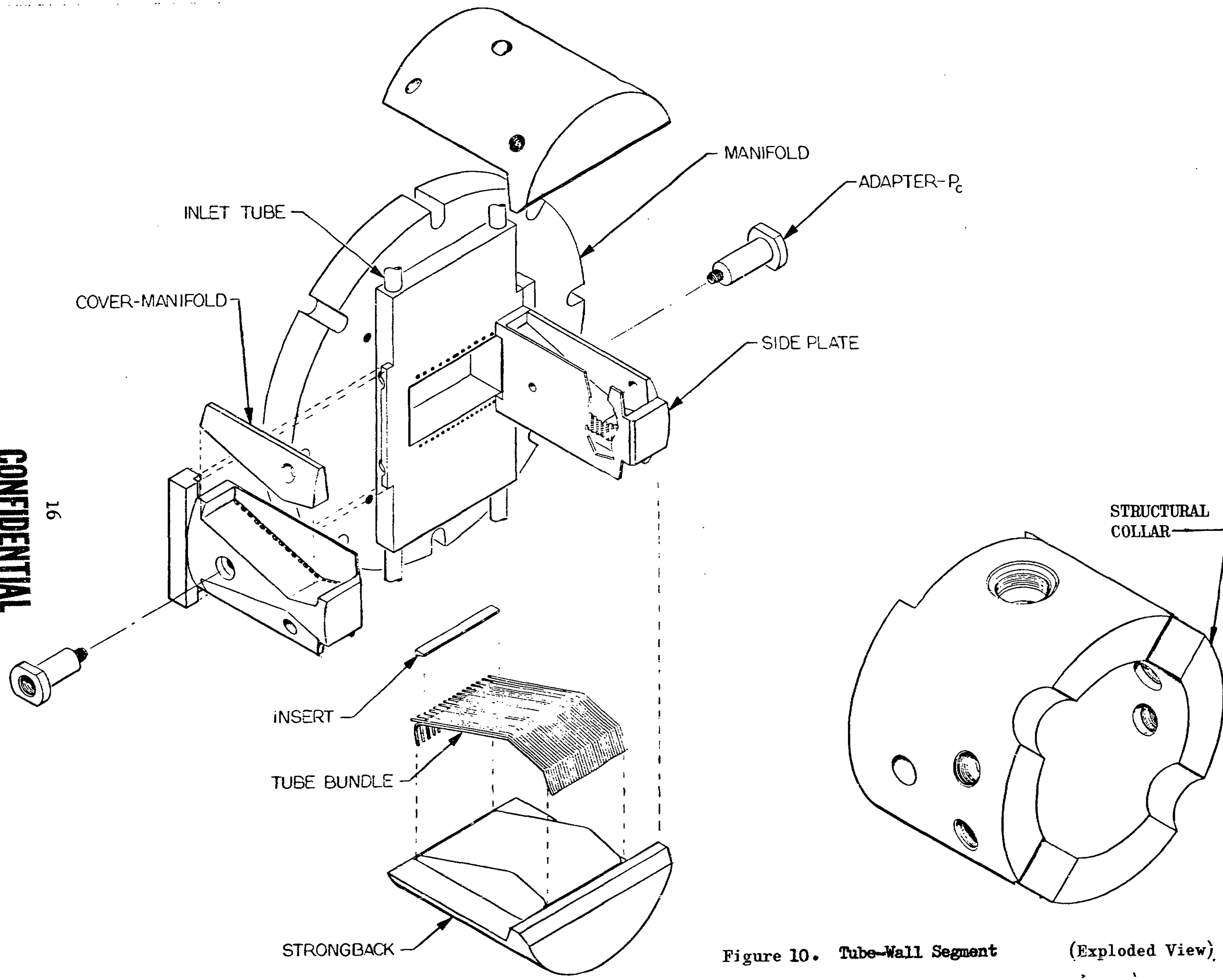

Figure 10. Tube-Wall Segment (Exploded View)

(U) A layout drawing of the rib segment is shown in Fig. 11. The segment design included a structurally simulated, nonoperational injector and tubes for the inner and outer walls. An isometric view of the composite segment is shown in Fig. 12. The rib and the honeycomb walls were assembled in a similar manner. The injector, side plates, and baffles were first assembled to provide the framework into which the panels (rib or honeycomb) were welded. The honeycomb material was used only as far as the throat which corresponded to the area over which the pressure load was applied. Three rib channels were added to the honeycomb panels downstream of the throat for similarity with the full rib panel to simulate the full extent of the outer wall. In addition to the full segments several samples were fabricated for each structural concept to develop fabrication methods.

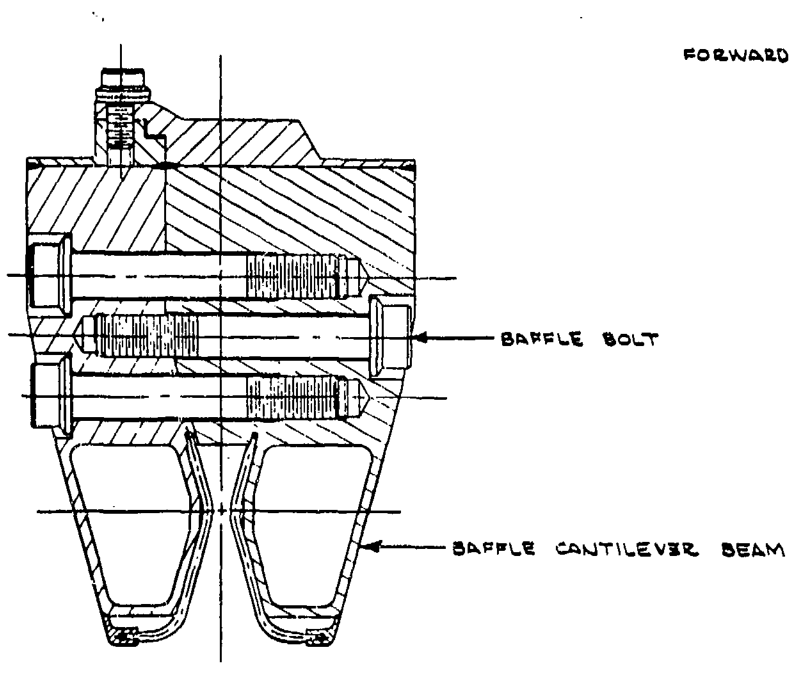

SECTION B-B

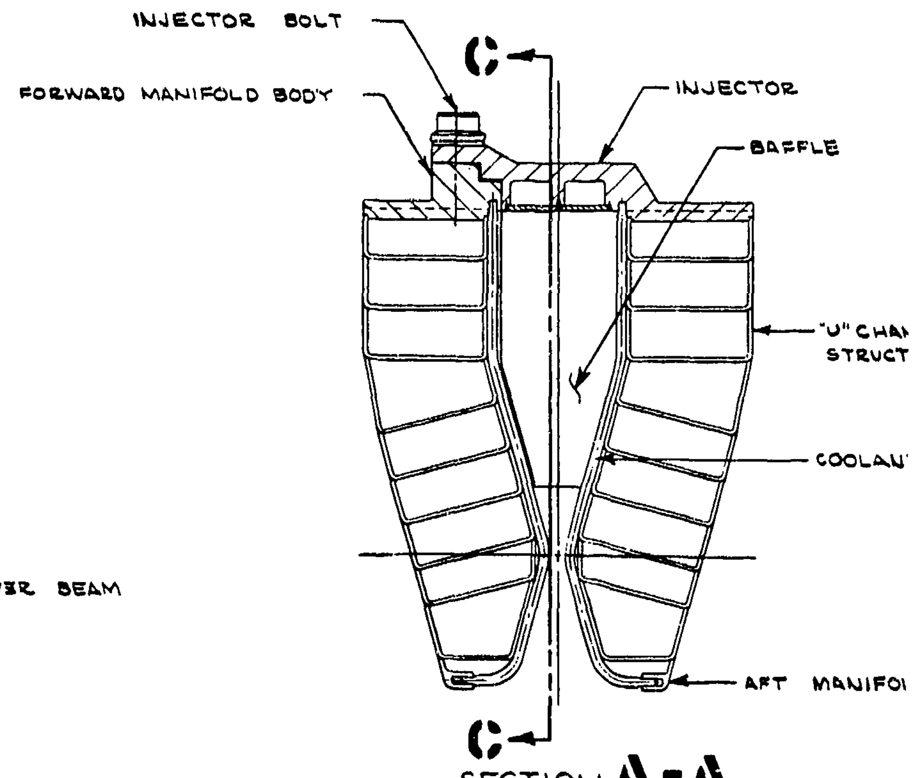

SECTION A-A

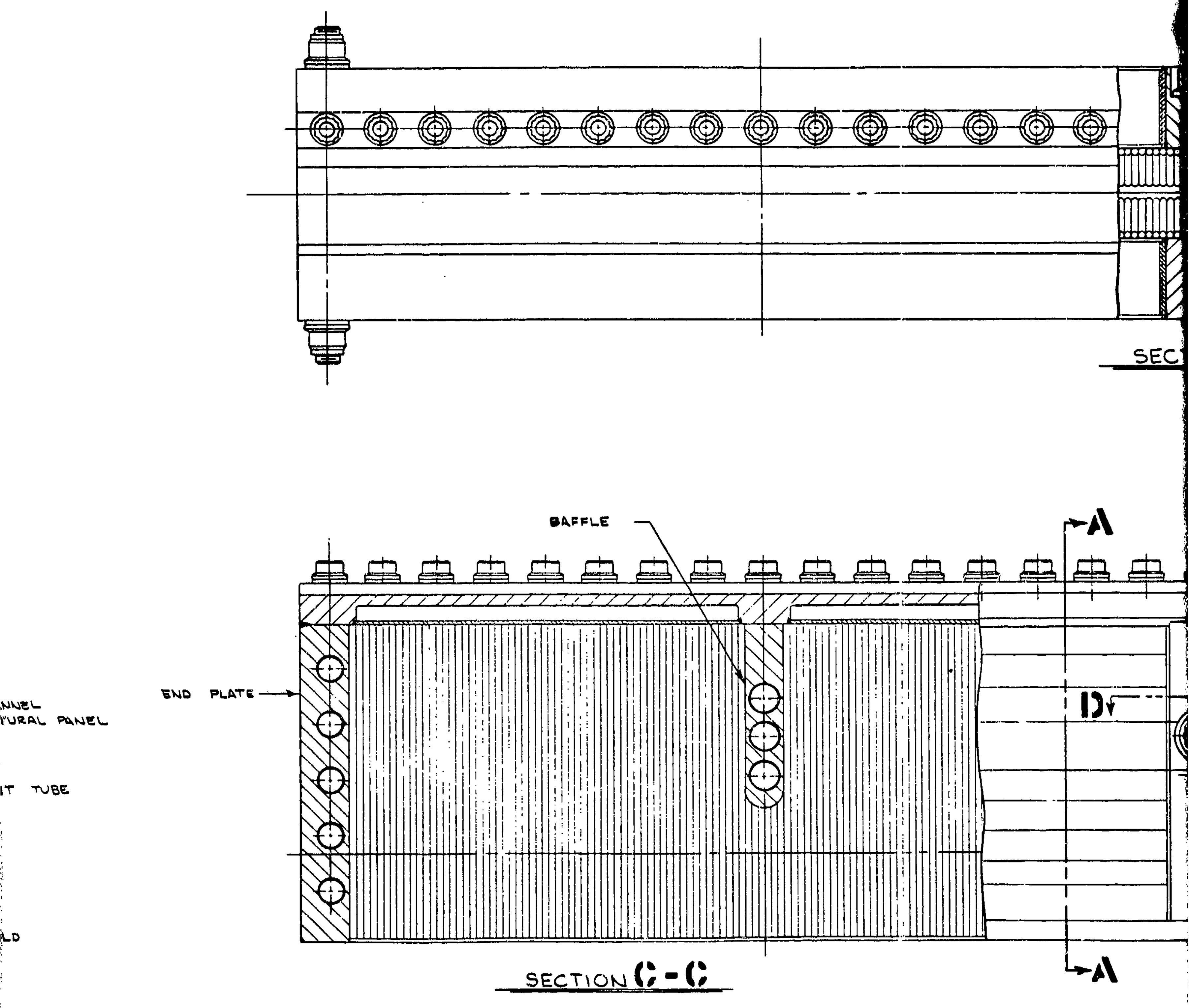

SEC
BAFFLE
A
END PLATE
NNEL
TURAL PANEL
IT TUBE
LD
D
SECTION C - C
A

Figure 11

2

CONFIDENTIAL

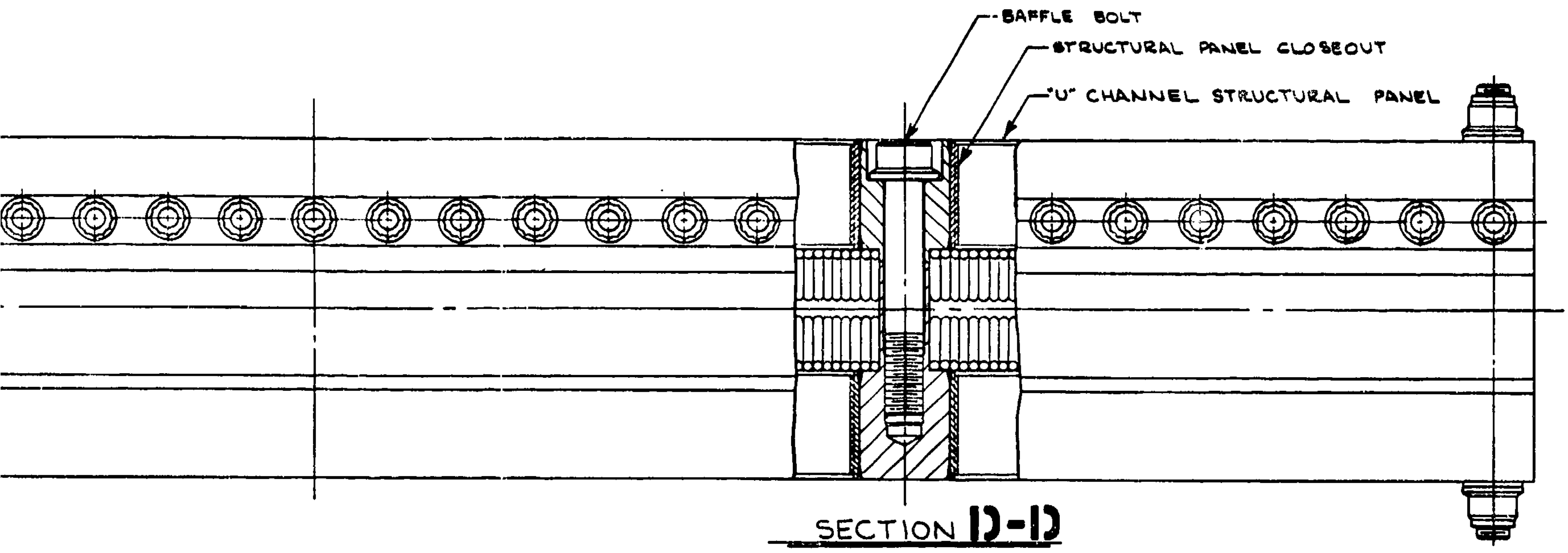

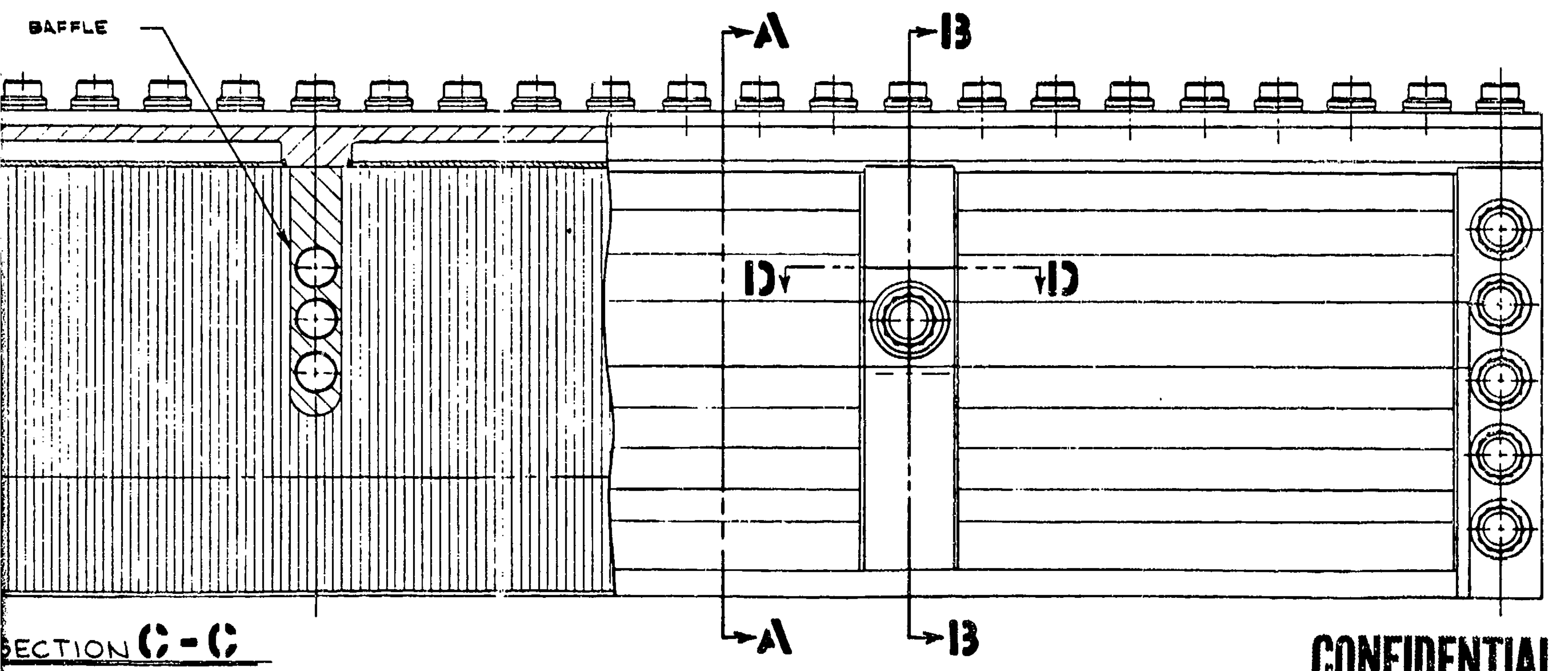

CONFIDENTIAL

Figure 11 Structural Test Segment - Rib Supports

3

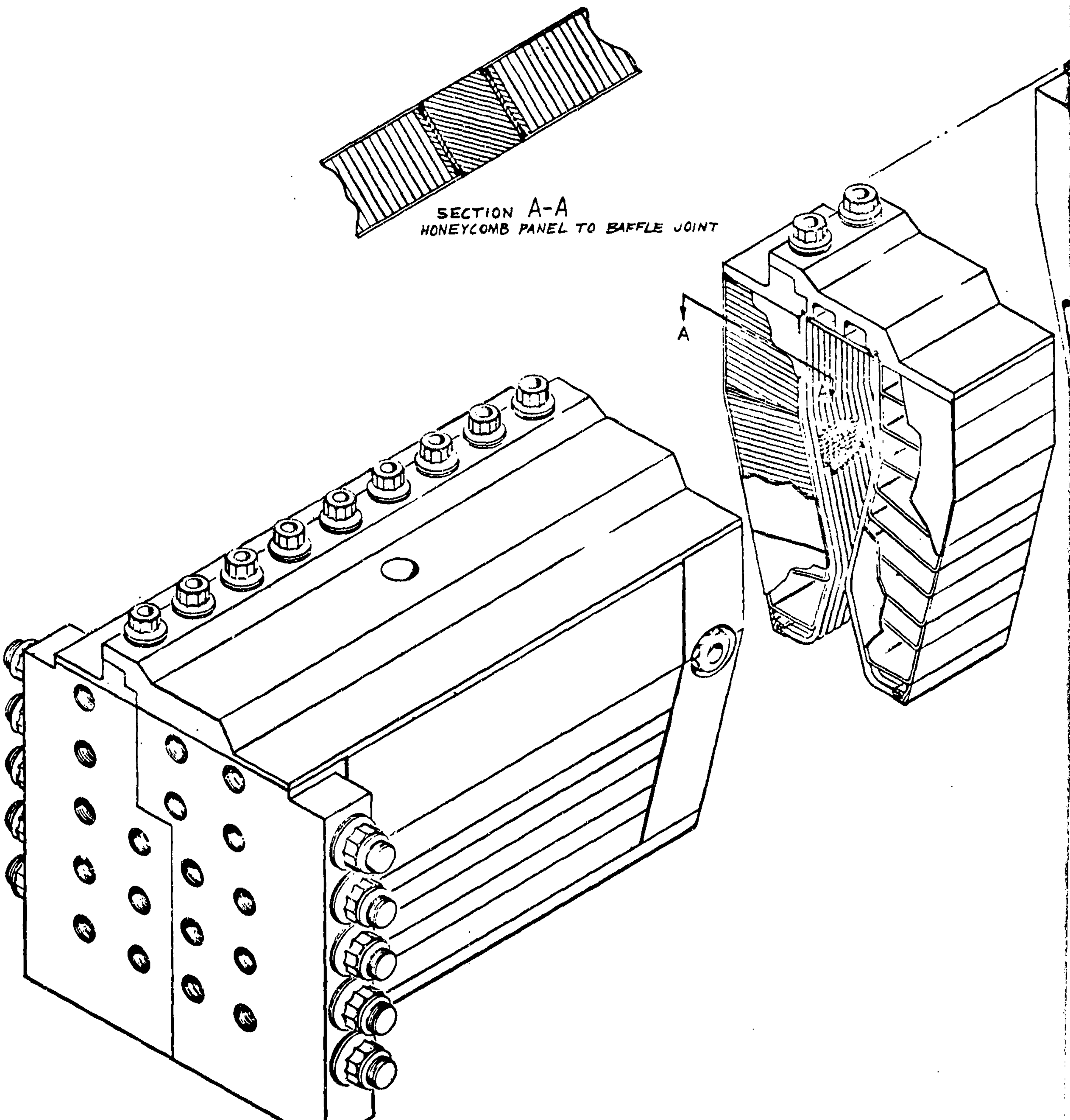
SECTION A-A
HONEYCOMB PANEL TO BAFFLE JOINT
A

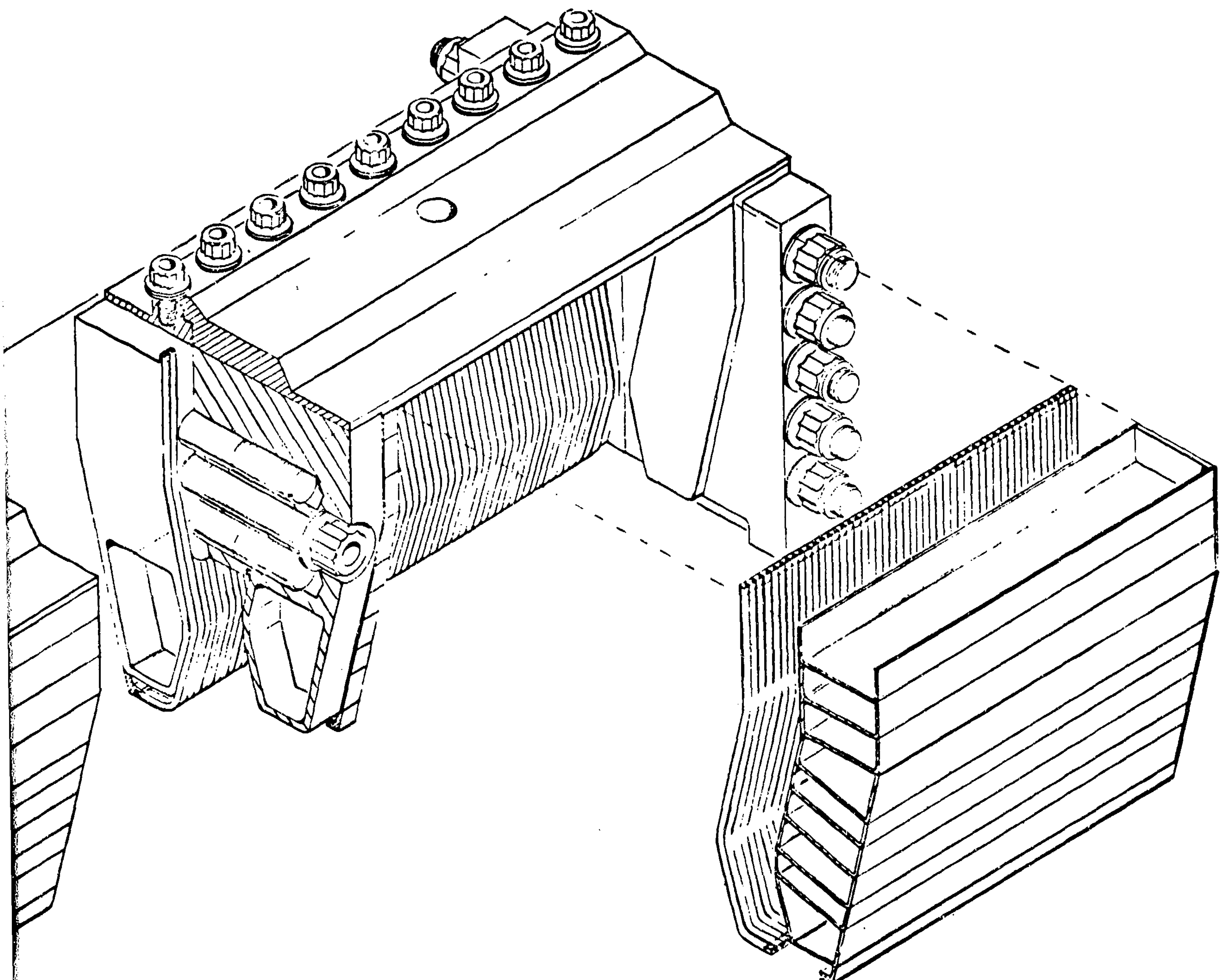

Figure 12 . Composite Rib/Honeycomb Structural Segment

CONFIDENTIAL

SECTION III

MATERIALS OF CONSTRUCTION

(U) Because of the similar requirements for the various segments, only a small number of different major construction materials were used. These included OFHC copper and nickel 200 for high conductivity applications and CRES 347 and Inconel 718 for structural elements. Various braze alloys were also used for the tube-wall inserts, the tube-wall segments, and the solid-wall segments.

1. OFHC COPPER

(U) The high conductivity of this material was required in the water-cooled hot-firing hardware to permit steady state operation with a relatively large spacing between the cooling passages to simplify the fabrication requirements as was shown in Fig. 4. Copper was used for all sections of the solid wall segments and for the injectors. Thermal analyses indicated that the copper would transfer heat from the injector face to the cryogenic liquid fluorine at a rate sufficient to prevent overheating of the face, and this was substantiated during the test program.

(U) Copper was used for the water-cooled portions of the tube-wall throat insert and also as the structural member of that component. Steel could have been used but sealing the numerous water passages at the interface of the core and collar was simplified by making a copper/silver eutectic bond at that surface.

(U) The water-cooled side walls of the tube-wall segment were made from OFHC copper because of its high thermal conductivity. The secondary structure behind the tube bundles and side walls (Fig. 10) was made of copper to simplify fabrication procedures but, as in the case of the throat inserts, a high strength material could have been used.

2. NICKEL 200

(U) Although the conductivity of nickel is less than that of OFHC copper, the higher strength (Table 2) of this material makes it preferable in several applications required in this program. Accordingly, the tubes for one of the tube-wall throat inserts and the two tube-wall segments were made of nickel. Thick wall tubes made by electroforming nickel on nickel tubes were fabricated as described in Section IV but were not assembled into a segment.

TABLE 2

COMPARISON OF NICKEL 200, OFHC COPPER, AND CRES 347

	Thermal Conductivity, Btu/in.-F-sec x 10^{-3}			Yield Strength, ksi		
	70 F	800 F	1800 F	70 F	800 F	1800 F
Nickel 200	1.00	0.63	0.82	22	16	2
OFHC Copper	5.10	4.86	-	9	2	-
CRES 347	0.20	0.28	0.38	39	32	9

(U) Nickel was electroformed on the edges of honeycomb core to provide a sufficient thickness of material for welding the core to the baffles and injector of the structural segment. Although the structural segments were tested at ambient temperature, nickel was used to be compatible with the operating conditions for a hot-firing engine where the walls would be heated. It was found that an improved braze bond was formed between the honeycomb core and the face sheets when a flash plating of nickel was applied to the core.

3. CRES 347

(U) This conventional tubing material was used for the tubes of one of the tube-wall throat inserts. As shown in Table 2, the strength of this material is superior to either copper or nickel, although the conductivity is quite low. The small diameter tubes used in the present application resulted in low tube wall stresses so that very high strength values were not significant because manufacturing tolerances dictated the minimum wall thickness. In the case of the CRES tubes, the maximum stress under design conditions were less than 6000 psi, whereas the tube strength was more than twice that value.

(U) CRES 347 was used as the structural shell for the tube-wall segments. It was also used for the forward end member of the segments which served as the hydrogen inlet manifold and adapter for the injector. The structural shell was shrunk fit on the copper core and welded to the forward manifold.

(U) The tubes for the structural segments were made of CRES 347. The outside diameter of these tubes was 0.093 inch and the thickness was 0.010 inch. The material and dimensions of these tubes were not critical since the segments were tested under ambient temperature conditions without the tubes to simulate hot firing conditions with nickel tubes in a plastic condition.

4. INCONEL 718

(U) This material was used extensively in the rib and honeycomb structural segments because of its high strength and low thermal expansion characteristics. The simulated injectors, baffles, and side plates were fabricated from 1/2-inch plate stock. The ribs, face sheets, and aft manifolds were 0.044-inch Inconel 718 sheet. Design analysis indicated that thinner material could have been used in some areas, but availability and fabrication simplicity resulted in the use of the 0.044-inch material.

(C) The honeycomb core had a hexagonal cell size (distance across flats of hexagon) of 0.125 inch. Cell walls were 0.004 inch thick. It was fabricated by first passing a 0.004 inch thick foil ribbon through a perforating machine which formed lines of tiny holes about 0.10 inch apart. These holes allowed venting of each cell during furnace brazing. The ribbon was then passed between corrugating wheels which formed three sides of the hexagonal cell. By resistance welding many such corrugated foil strips together, a honeycomb core section was built up.

(C) The necessary honeycomb core density was determined by the maximum shear loads at the panel to baffle junction. No attempt was made to vary core density below that necessary at the panel edges, but in an engine panel the core foil thickness could be linearly tapered by chemical milling to near zero at the panel center. Calculations indicated a required maximum core density of 35 lb/cu ft. The density of the delivered core sections was 40.1 lb/cu ft. While many combinations of cell size and foil ribbon thickness would produce the necessary core density, a cell size greater than 0.125 inch would not provide enough braze fillet area in contact with the face sheets to prevent delamination.

5. BRAZE MATERIALS

(U) The alloys listed in Table 3 were used to join the copper elements of the solid- and tube-wall segments, to bond the tubes to the support members, and to bond the face sheets to the honeycomb core as indicated. Further details of the areas brazed and the techniques used are discussed in Sections II and IV. These alloys were applied in the forms of foil, paste, or wire depending on the configuration of the particular areas being brazed.

TABLE 3

BRAZE ALLOYS USED IN SEGMENT FABRICATION

Alloy	Composition	Brazing Temperature, F	Elements Brazed
Nicoro	3-Ni/62-Cu/35Au	1900	TWI and TWS: tubes to support structure
50/50	50-Ag/50-Cu	1800	SWS and TWI: side walls to contour walls; TWS: strongbacks (tube support) to inlet manifold, side plates and inserts to tubes and inlet manifold
Eutectic	Ag/Cu	1500	SWS and TWS: core to collar
BT	72-Ag/28-Cu	1450	SWS and TWS: hydrogen and water coolant inlet tubes to collar
Palniro	8-Pd/22-Ni/70-Au	1950	HS: face sheets to core

SWS - Solid-wall segment
TWI - Tube-wall throat insert
TWS - Tube-wall segment
HS - Honeycomb segment

SECTION IV

FABRICATION PROCESSES

(U) During the course of fabricating the segments described in Section II, several special processes were used. In instances where techniques had to be developed or materials selected, evaluations were first accomplished with samples of the final item. These sample evaluations, as well as the final fabrication processes, are described in this section. The processes of interest included electrodeposition, electrodischarge machining, brazing, welding, and heat treating.

1. ELECTROPLATING

a. Surface Protection

(C) Electroplating was employed on the solid-wall segment throat sections to protect the copper wall from the hot products of combustion. Two materials were plated onto the copper surface. A 0.0003-inch thick layer of chromium was first used. Although it presented a satisfactory appearance afte, plating, the chromium did not adhere well, and a substantial portion of it was gone after a hot-firing test of a few seconds duration A plating of nickel 0.001 inch thick was applied to another copper throat section. The results of seven tests with this plated throat section indicated good adherence of the nickel to the copper.

b. Surface Preparation for Brazing

(U) In order to obtain a leakproof joint between the core and collar assemblies of the tube-wall throat insert, a copper/silver eutectic bond was made between the two elements. A 0.0015-inch layer of silver was plated on the outside diameter of the core, and the two parts were joined together as described in the brazing section of this report. No problems were encountered during this plating operation, and good joints were generally obtained.

(U) Nickel plating was also used to prepare the honeycomb material of the honeycomb structural segment for brazing to the face sheets. The honeycomb and the face sheets were both Inconel 718, and the braze alloy was Palniro 7. Samples of core material were brazed to the face sheets with and without a flash plating of nickel. The nickel plated core sample indicated superior wetting and fillet qualities over the sample indicated superior wetting and fillet qualities over the unplated sample. The cores of the final fabricated honeycomb structural segment were, therefore, flash plated with nickel prior to brazing.

2. ELECTROFORMING

a. Honeycomb Edge Forming

(U) In order to transmit shear loads from the honeycomb core to the baffles and injector, a shear joint must be formed directly between these members. In more lightly loaded structure, this joint is usually brazed, and some percentages of the braze joint is usually cracked by distortion as the panel is welded into surrounding structure. As this joint is very difficult to x-ray or repair after assembly in the honeycomb segment, it was considered safer to substitute a relatively deep electron beam weld between baffle or injector and honeycomb. However, the thin gage honeycomb cannot be welded to these thick sections directly. A thick layer of nickel was, therefore, electroformed on the edges of the core sections to form a good weld base. This approach was verified by sample welds before assembly of the segment was started.

(U) The sample was an Inconel 718 block with V-shaped notches machined on one surface to simulate the edge or open cells of the honeycomb core. During plating, the nickel deposited more rapidly on the raised edges and would eventually tend to form inclusions as shown in Fig. 13. These inclusions would be detrimental during the subsequent braze operation and would weaken the joint. To prevent the inclusions, the nickel was electroformed, machined to a flat surface with small depressions, re-electroformed, and remachined to a flat surface as shown in Fig. 13.

(U) A complete honeycomb sample panel was made using this process and indicated that three cycles would be required to obtain a perfectly smooth surface. Two of the honeycomb cores, masked with Plexiglas, are shown in Fig. 14. A total plating time of 250 hours was required to obtain a maximum depth of 0.250 inch. One of the final honeycomb panels which used this electroforming process is shown in Fig. 15 after the final machining of the nickel edges.

b. Electrodeposition Coating of Tubes

(C) Conventional regeneratively cooled thrust chamber tubes normally re-require tapering to vary the inside diameter, forming to the desired combustion chamber contour, and flattening so the tubes have a constant width. To improve the tube design, tapered tubes were evaluated in which either the throat region or the complete tube was plated and then ground to a constant outside diameter. This concept reduced the number of tubes required for a given chamber circumferential length, L, and result in larger size tubes for a given total coolant flowrate. The tube concepts are illustrated in Fig. 16.

(C) 347 CRES Tubes Coated With Copper. A number of 347 CRES tube samples over which a sheath of copper was electrodeposited were evaluated for purity of the plating and adherence of the copper to the CRES surface. A requirement that the plating meet oxygen free high conductivity copper (OFHC) standards was considered mandatory for successful braze operations in assembling a thrust chamber. A "tight" interface between

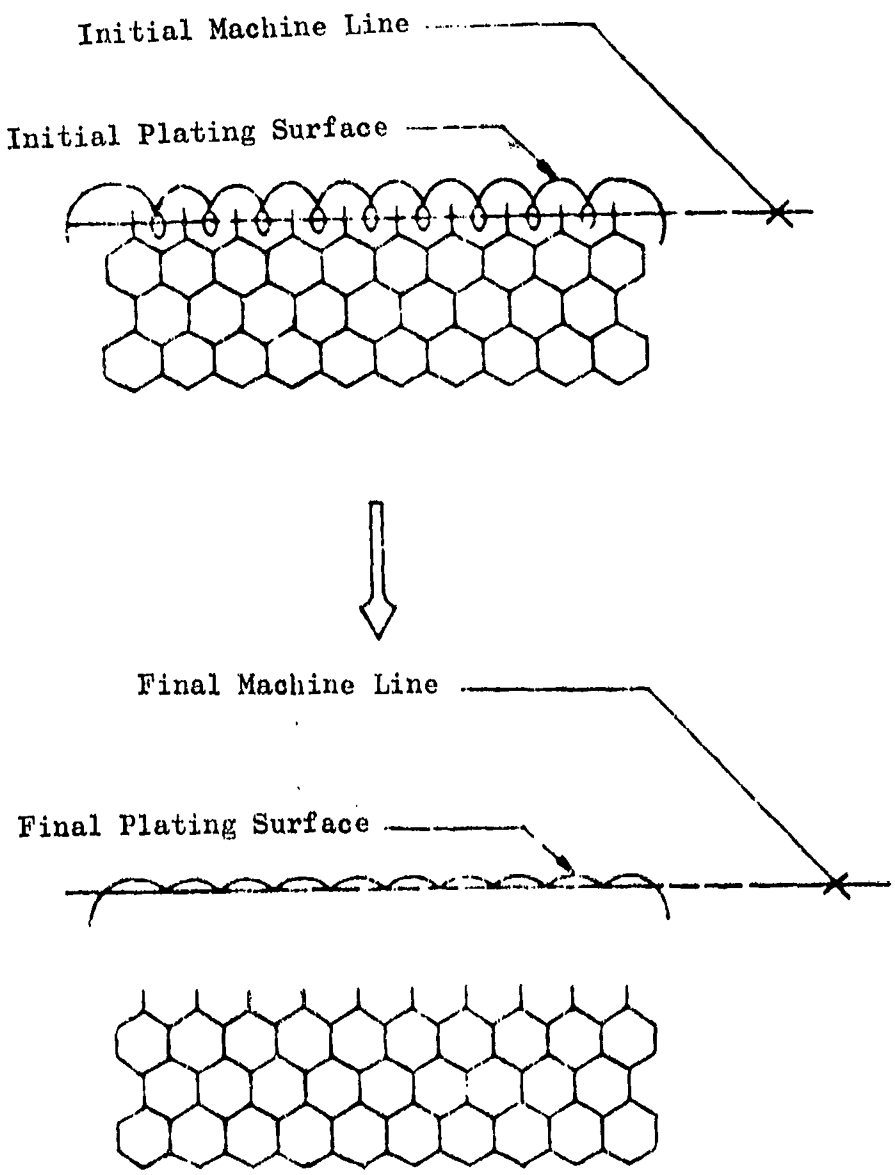

Figure 13. Honeycomb Edge Plating Sample

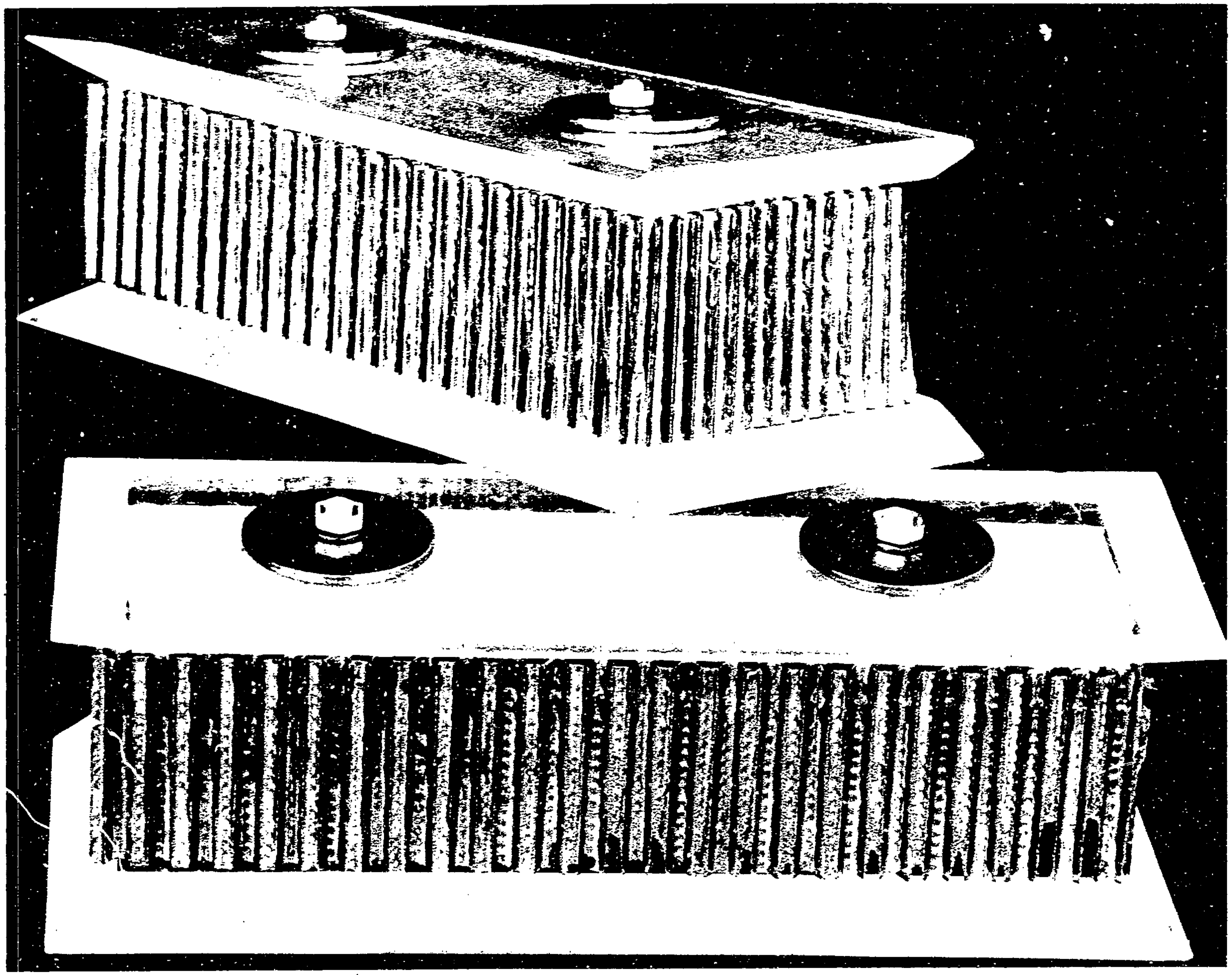

Figure 14 . Honeycomb Panels and Masks Prior to Nickel Plating

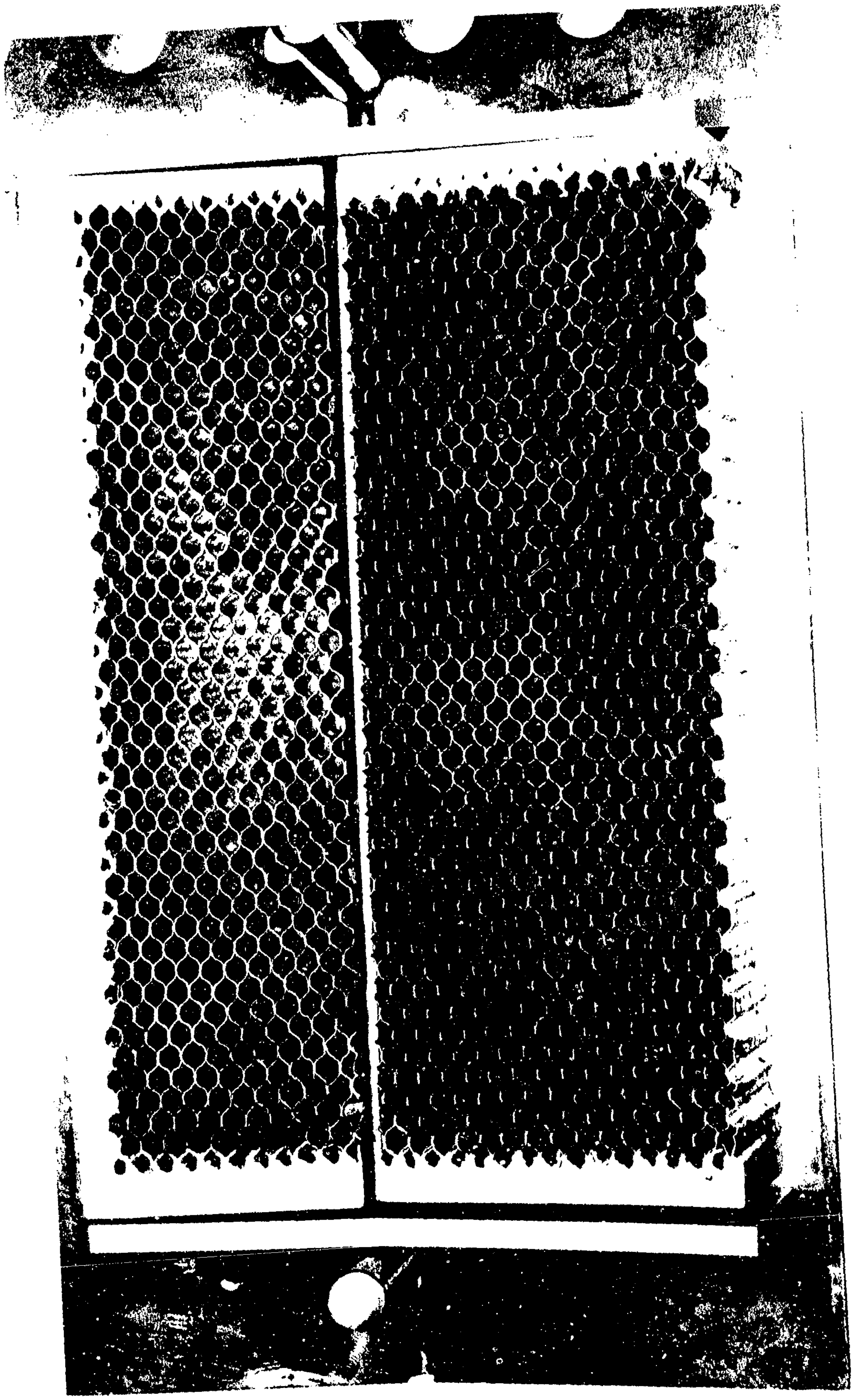

Figure 15. Plated Honeycomb Cores & Closeouts in Formblock

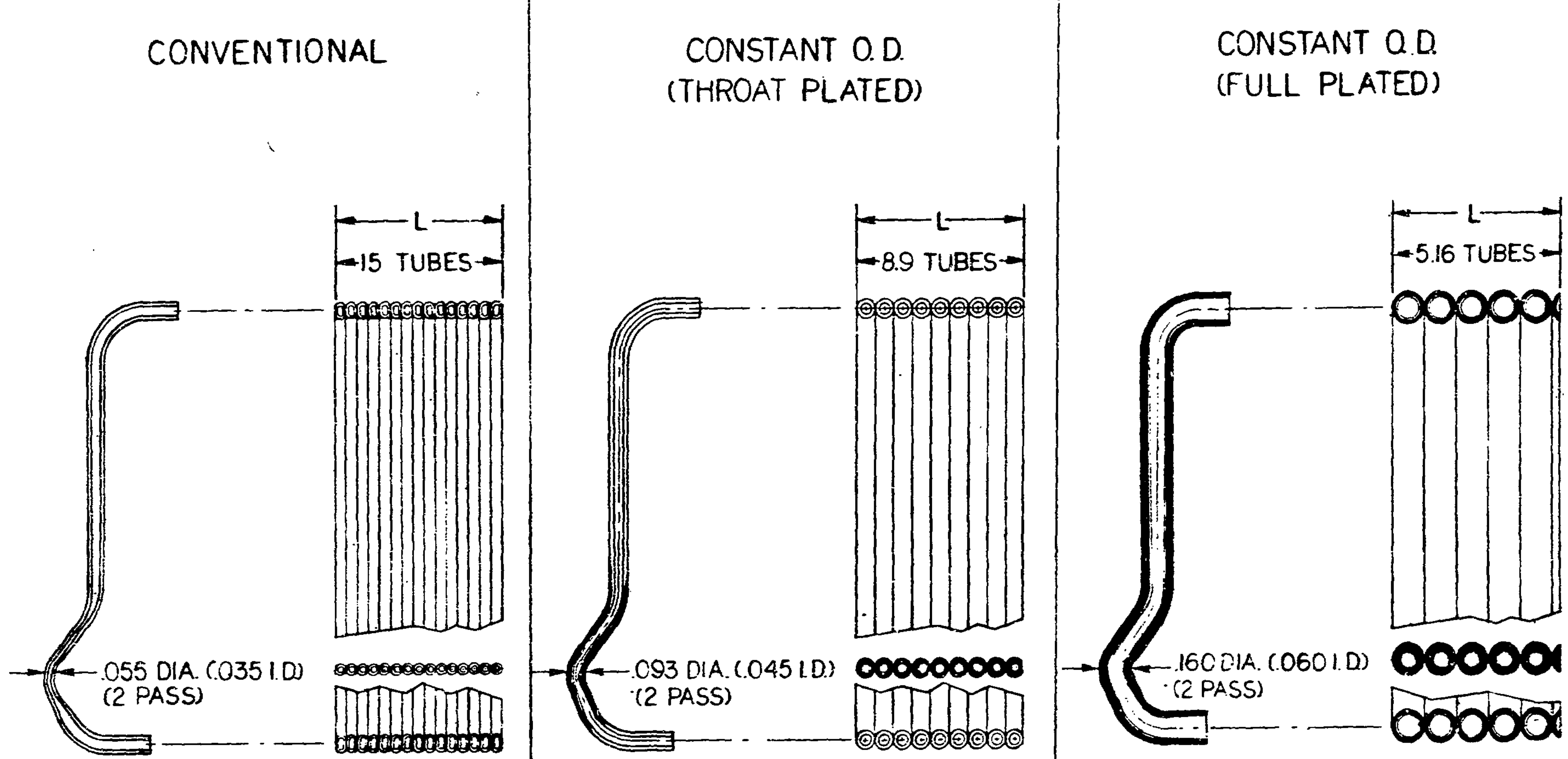

Figure 16. Comparison of Plated and Conventional Tubes

the copper and the CRES was also considered necessary for good conduction of heat from the copper into the CRES during chamber operation. The original CRES tubes were 0.098 inch in diameter.

(U) Laboratory Analysis. As-received (as-deposited) metallographic specimens were removed from the areas shown in Fig. 17. The remaining sections of the specimen were exposed to a standard hydrogen embrittlement test for OFHC copper. This test consists of exposing the specimens to a temperature of 1800 to 1850 F for 4 hours in an atmosphere of dry hydrogen (-70 F dewpoint or lower) and then rapidly cooling the specimens. Metallographic specimens were then removed from the sections as shown in Fig. 17.

(C) Visual examination of the as-deposited copper surface of the specimen revealed a rough texture with evidence of transverse surface cracks in the copper. Metallographic examination disclosed a large columnar grain configuration in the copper sheath as shown in Fig. 18 and 19. The interface bond was good as shown in Fig. 20. The surface of the copper was very rough with some areas having a difference of 0.00095 inch in height between low and high spots. The depth of copper deposit as measured on the various specimens is tabulated in Fig. 17. Intergranular cracks as shown in Fig. 21 were observed with a maximum depth of 0.0094 inch.

(U) Visual examination of the copper surface on the specimens exposed to the hydrogen embrittlement test showed no evidence of blistering. The surfaces as shown in Fig. 22 and 23 were identical with those observed on the as-deposited specimens examined. Metallographic examination of the exposed specimens revealed a duplex grain structure typical of copper which is exposed to temperatures above the recrystallization temperature (Fig. 23). It should be noted, however, that the grain growth was not as pronounced as it normally is in OFHC copper. Metallurgical examination also disclosed heavy out gassing indicative of hydrogen embrittlement. The severity of the voids observed is shown in Fig. 24. The micro voids resulted from the reaction of hydrogen with oxides present in the copper prior to the embrittlement test. Metallurgical evaluation of a longitudinal section through the specimen disclosed surface cracking with a maximum depth of 0.0061 inch as shown in Fig. 25. These cracks had an intergranular character and were identical with the other cracks previously reported.

(U) The cracking observed on the surface of the copper sheath indicated brittleness and high residual stress due to plating rate. There was no evidence of any connection between the cracking and the gassing caused by exposure of the copper in a hydrogen atmosphere. The gassing is indicative of copper which is not oxygen free. The amount of gassing present in the metallurgical specimens evaluated was considered to be marginally unacceptable for subsequent braze processes.

(C) Braze Samples. To further evaluate the acceptability or nonacceptability of the tubes for brazing, three pieces of tubing were furnace brazed together on a 347 CRES base plate. The tubing was approximately 0.165 OD with a range of copper plating from approximately 0.010 to 0.045 on 347 CRES tubing. The resulting test assembly

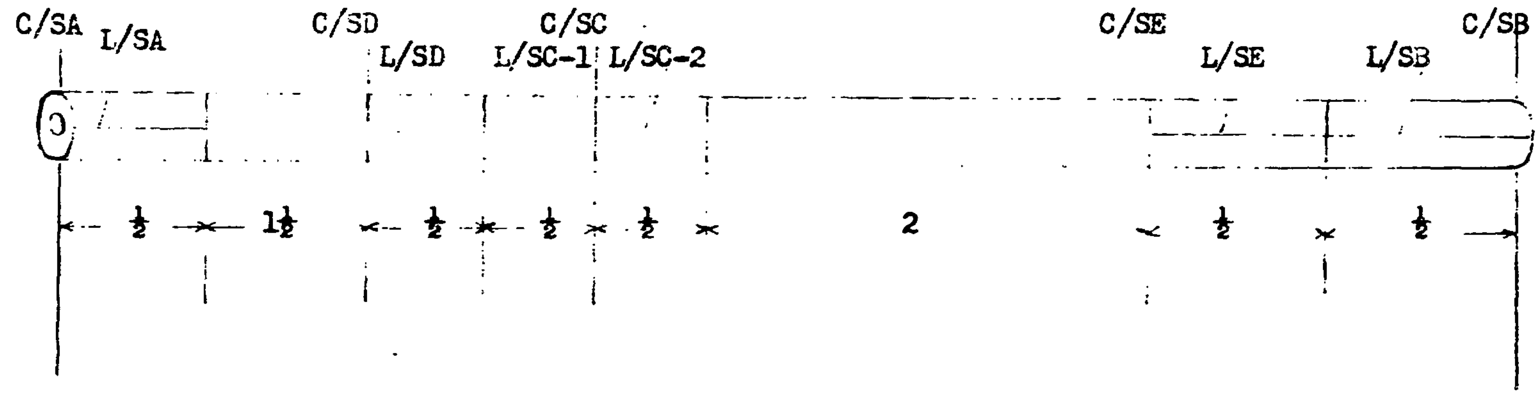

Specimen	Condition	Copper Depth Max.	Copper Depth Min.	Vickers Hardness VDPF 500 gram Load
C/S A	As Deposited	0.0208"	0.0184"	VDPH 52.3 to VDPH 66.8
L/S A	As Deposited	0.0180"	0.0180"	
C/S B	As Deposited	0.0184"	0.0180"	VDPH 54.7 to VDPH 62.3
L/S B	As Deposited	0.0184"	0.0180"	
C/S C	As Deposited	0.0184"	0.0184"	
L/S C-1	As Deposited	0.0203"	0.0189"	
L/S C-2	As Deposited	0.0194"	0.0184"	
C/S D	Exposed to H_2	0.0199"	0.0184"	VDPH 53.6 to VDPH 62.3
L/S D	Exposed to H_2	0.0194"	0.0189"	
C/S E	Exposed to H_2	0.0189"	0.0180"	VDPH 53.2 to VDPH 65
L/S E	Exposed to H_2	0.0194"	0.0184"	

Figure 17. ***Location of Metallographic Specimens Removed From Electroformed Copper-347 CRES Tube***

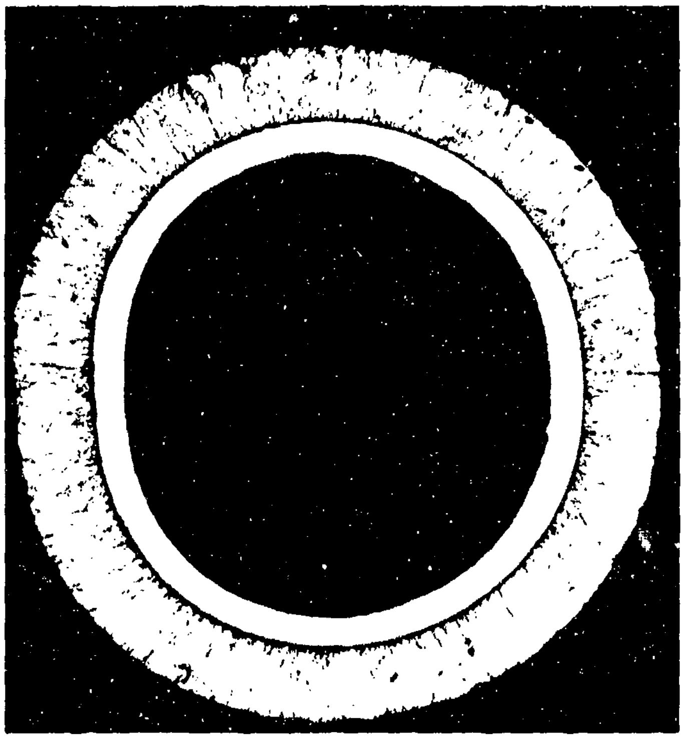

Figure 18. Typical Cross-Section of 347 CRES Tube With Electroformed Copper Sheath on OD.

Mag. 20X

Figure 19. Typical Microstructure of "As-Deposited" Electroformed Copper Sheath

Mag. 100X

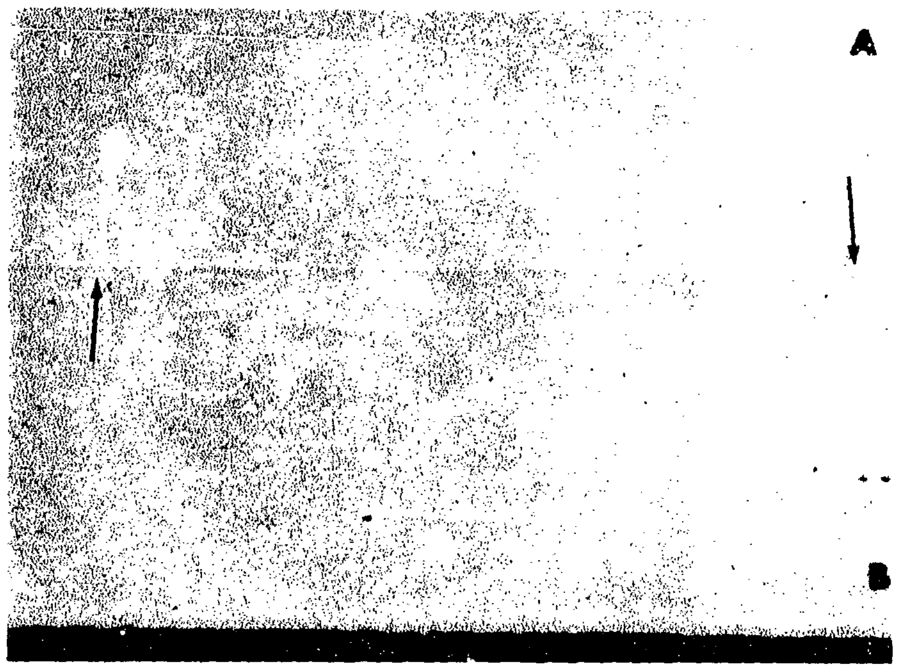

Figure 20. Typical Interface (Arrows) between Copper A and 347 CRES B in "As-Deposited" Condition.

Mag. 200X

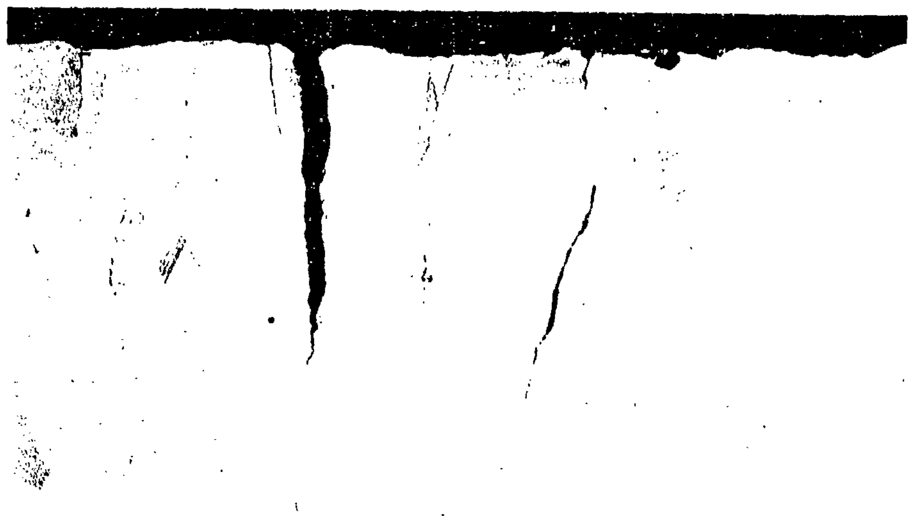

Figure 21. Typical Radial Cracks Observed in As-Deposited Copper Sheath.

M 200X

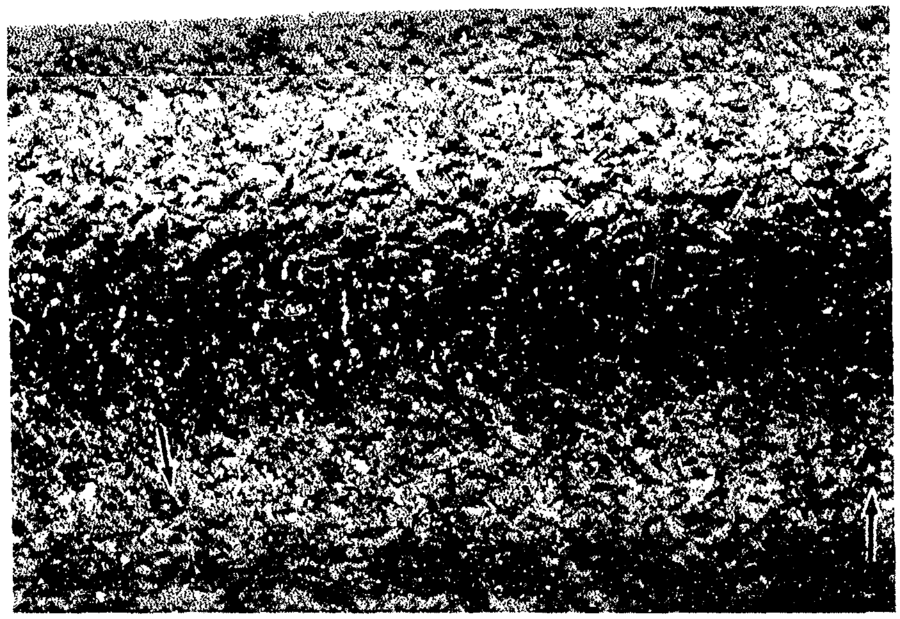

Figure 22. OD Surface of Copper Sheath.

Mag. 20X

Figure 23. Typical Cross-Section Through Tube Section with Copper Sheath After Exposure to Hydrogen Embrittlement Test.

Mag. 20X

Figure 24. High Magnification Photomicrograph of Section Showing Gassing (Spherical Voids)

Mag. 200X

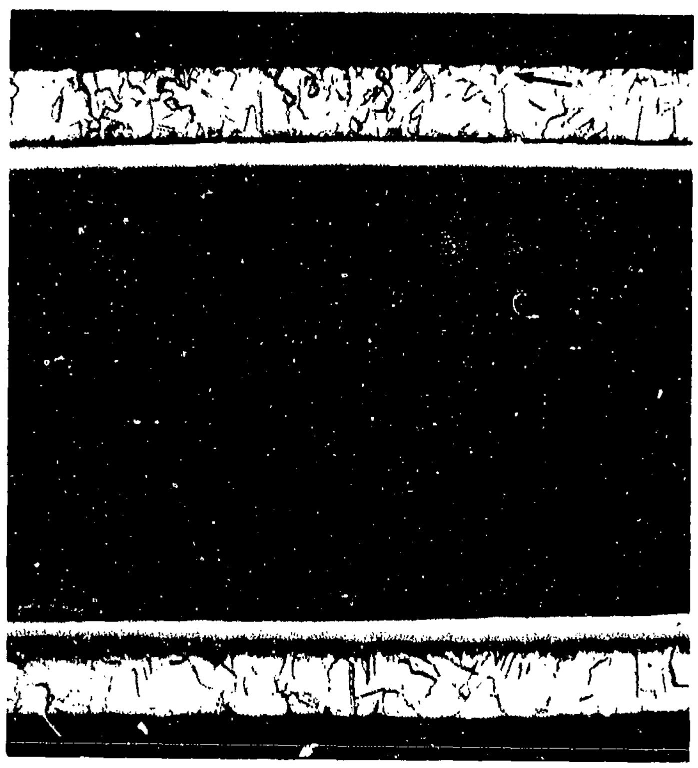

Figure 25. Typical Longitudinal Section

Mag. 20X

showed noticeable blister type deformation on the thinnest plated specimen. These blisters varied in size with the larger one being approximately 0.040 diameter at the base. The two remaining tubes had small patches of microscopic blisters (Fig. 26 and 27). The blisters were attributed to the impurities in the copper plating. A lower temperature braze cycle could possibly help alleviate the stringent requirement on the purity of the copper.

(C) Thermal Conductivity Tests. A copper plated stainless steel tube was used as a heat transfer test section in order to evaluate the quality of copper plating and resistance to heat transfer at the copper-stainless steel interface. The copper plated tube was instrumented with thermocouples and voltage taps for temperature and power measurements as shown in Fig. 28. Bus bars for electrical heating were brazed on. It was then placed in a helium flow system, and six experiments were performed.

(C) For the given experimental conditions, the tube inner-wall temperatures were calculated by two methods. The first method involved the use of a previously developed helium heat transfer correlation. The second method utilized the measured outer wall temperature and the conduction drop through the bimetallic tube wall. The two calculated temperatures were then compared and utilized as an indication of the quality of the copper plating and copper-stainless steel interface resistance.

(C) The temperatures calculated from the thermal properties of the wall were in most cases slightly higher than those calculated from the heat transfer correlation, inferring possible degradation of the thermal conductivity of the copper due to the plating process and resistance to heat transfer at the bimetallic interface. The small amount of degradation of thermal conductivity inferred from the results could not be evaluated exactly due to allowable variations in the heat transfer correlation utilized. Therefore, it was generally concluded that the heat transfer through the composite copper and stainless steel walls of the bimetallic test section indicated temperature drops which would be approximately expected from the pure materials.

(C) Nickel Tubes Coated With Nickel. A second constant outside diameter tube concept was also evaluated. The concept was similar to that described above but utilized tapered nickel tubes upon which a sheath of nickel was deposited. The tubes were then ground to a constant outside diameter of 0.093 inch. Successful application of this concept was made to electroforming the ends of a tube bundle for insertion into a rectangular slot.

(C) Tapered Tube Coated With Nickel. Sample tubes were successfully plated in which good adherence and purity of the plating were obtained. A cross section of a typical tube magnified 200 times is shown in Fig. 29. Plated tube samples were also successfully brazed together and to a backup structure with no indications of the blistering experienced previously with the copper plated CRES tubes.

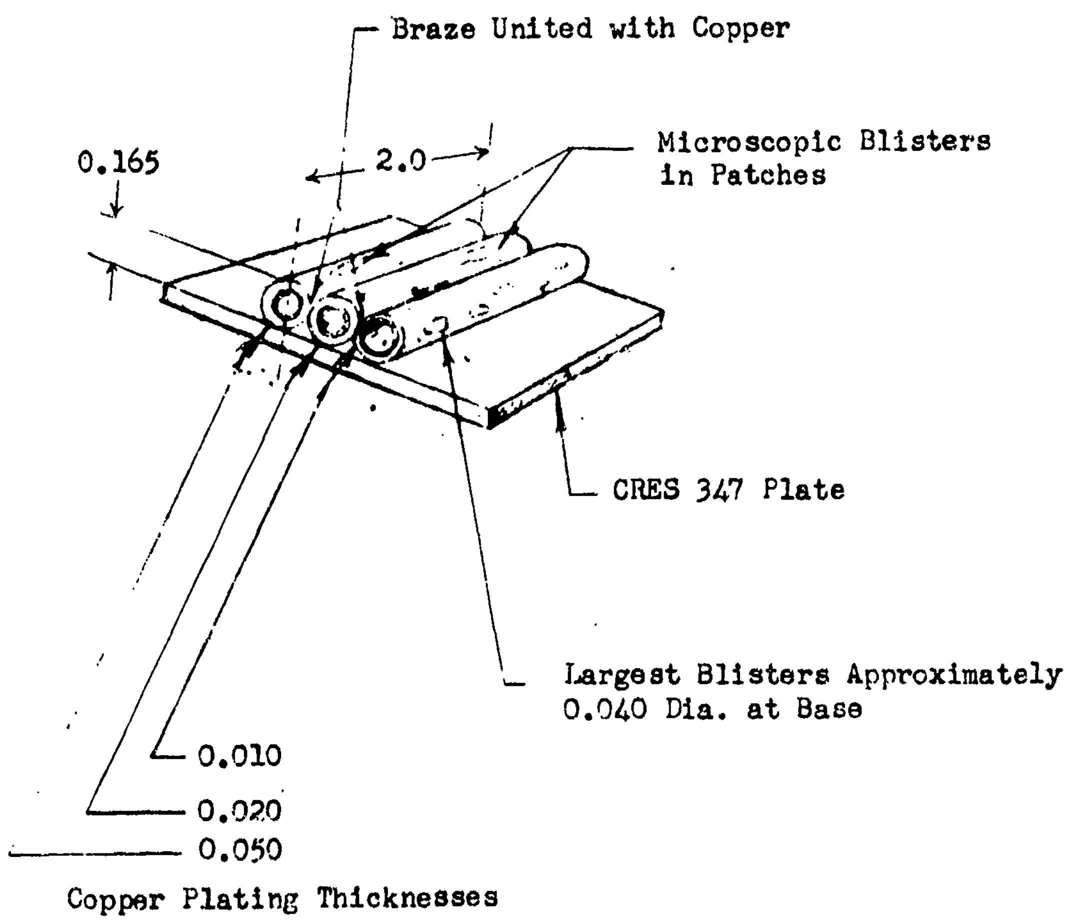

Figure 26. Significant Features on Brazed Tube Sample

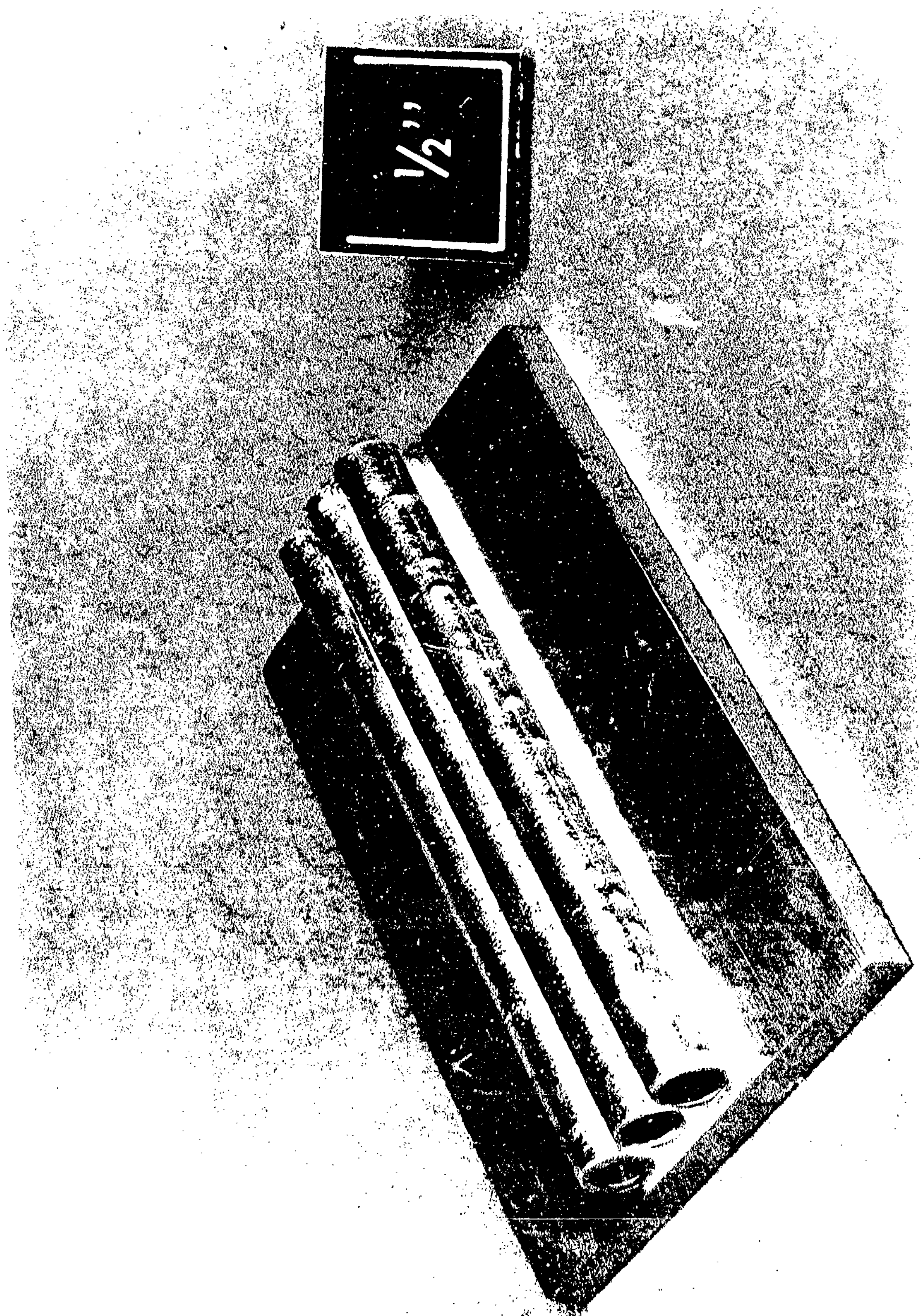

Figure 27. Brazed Copper-Plated CRES Tubes

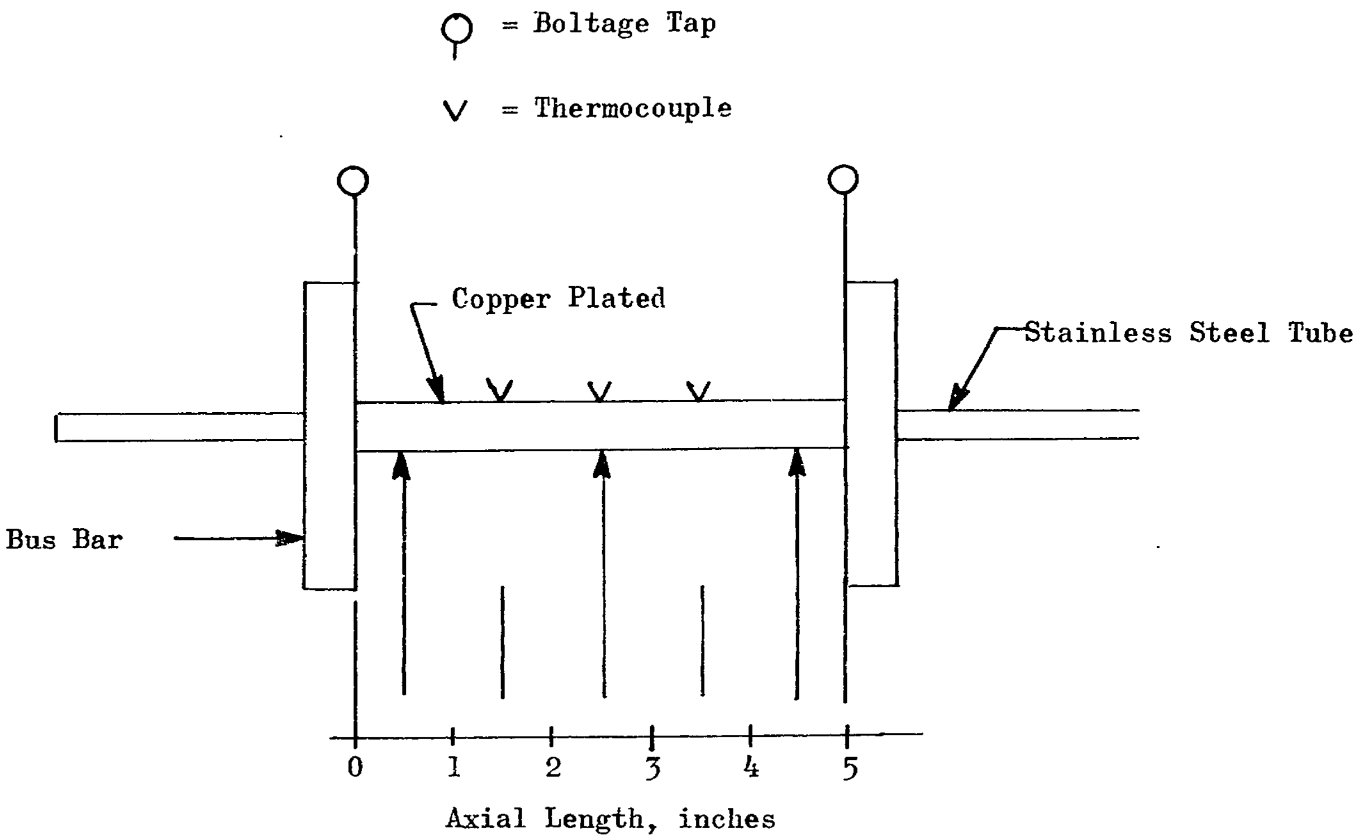

OD Overall	0.246 inch
Copper Thickness	0.052 inch
Stainless Steel Thickness	0.010 inch
Tube ID	0.142 inch

Figure 28. Schematic of Bimetallic Test Section

Figure 29. Cross Section of Nickel-Plated Tube (200X)

(C) When fabrication of a larger number of tubes was attempted, however, a problem of holding concentricity of the tubes during the centerless grinding process was encountered. The nonconcentricity of some of the tubes resulted in varying wall thicknesses such that the strength and heat transfer of these tubes could be adversely affected when assembled into a thrust chamber. An x-ray photograph of an assembled tube bank in which some of the tubes were nonconcentric is shown in Fig. 30.

(C) During the electroforming process the tubes deformed slightly. These nonstraight tubes could not then be ground accurately by the centerless grinding process. It was concluded that the electroforming and grinding method was not satisfactory for this application. To obtain constant OD variable ID tubes it would be necessary to procure thick wall tubes, taper to the inside contour, and grind to the constant OD. Because of the long procurement time for this tube material, it could not be accomplished during the subject program.

(U) Tube Bundle End Forming. For the hot firing tube-wall hardware, hydrogen coolant enters the tubes from manifolds and is collected in manifolds after leaving the tubes as shown in Fig. 6 and 10. The tube bundle enters the manifold through a rectangular slot in the manifold. The interstices between the circular tubes present relatively large void areas which must be filled during the brazing operation which seals the tubes-to-manifold joint. The area of the interstices could be greatly reduced for thin-walled tubes by compressing the ends of the tube bundle so that the tubes become nearly square in cross section. This process is not applicable to thick-wall tubes because of the reduction of flow area which would result.

(U) The interstices were eliminated completely on the tube-wall segment by electroforming a sufficient thickness of nickel onto the ends of the nickel tube bundle such that the surface could be machined to a constant thickness rectangular cross section as shown in Fig. 31. Brazing of these end-formed tube bundles into manifolds was accomplished without any instances of leakage at the joint.

3. ELECTRODISCHARGE MACHINING

a. Surface Forming

(U) This process was employed to form the contour of the solid-wall segment throat sections. Conventional machining of these areas would have been very difficult as indicated by the detail of the throat and chamber contours as shown in Fig. 2 and 4. For the first nozzle, the electrodischarge machining operation was performed prior to the drilling of the coolant water passages. The close proximity of these passages to the surface (0.070 inch) resulted in slight surface deformations. Subsequent nozzles were fabricated by drilling the holes prior to the formation of the contour. Surface deformations during fabrication were eliminated by this sequence of operations.

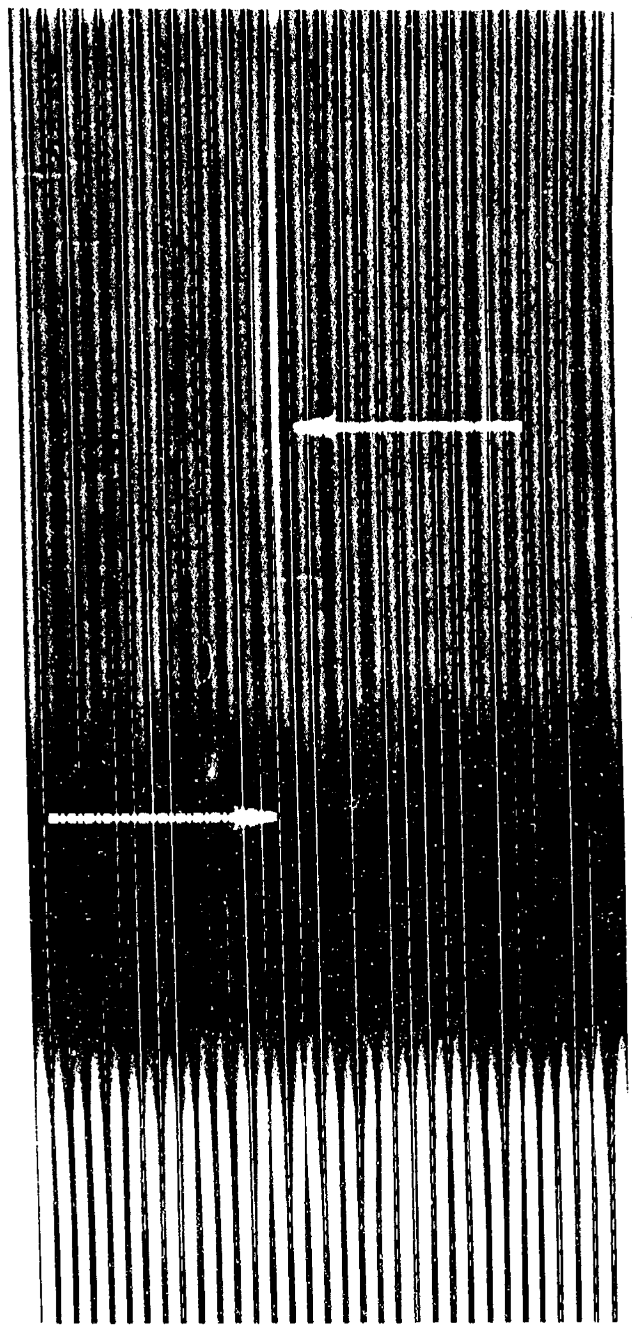

Figure 30. Tube Bank Showing Nonconcentric Tubes

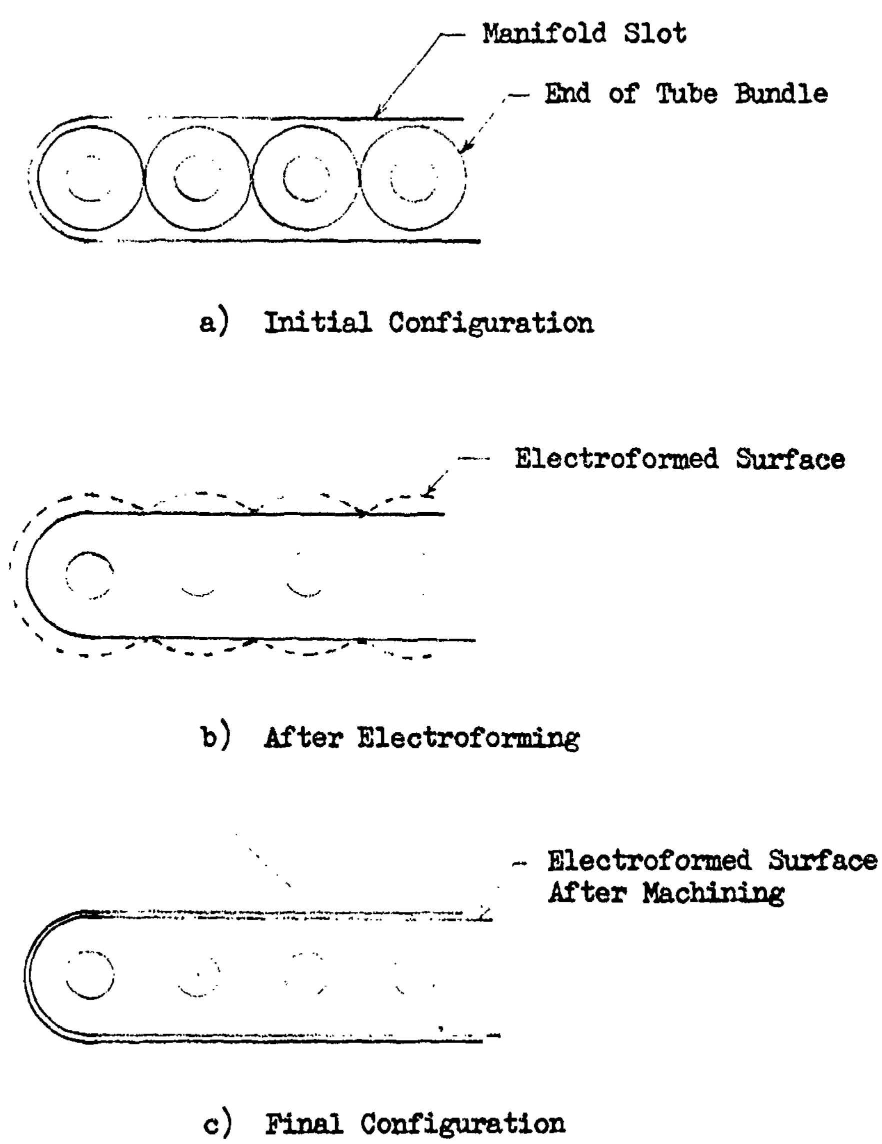

Figure 31. Joint Between Tube Bundle and Manifold

b. Small Hole Boring

(C) Another use of electrodischarge machining was a preliminary investigation of methods of obtaining small holes in the walls of coolant tubes. The tubes used were made of CRES 347 and nickel 200. The wall thicknesses for these two materials were 0.012 and 0.024 inch, respectively. It was desirable to have a small angle between the axes of the hole and the tube. This results in large values of the ratio of the hole length to hole diameter, L/D, which increases the difficulty of drilling such a hole because conventional drill bits tend to bind, flex, and break under these conditions.

(C) For comparison with the electrodischarge drilling method, a mechanical drilling operation was used. This operation, called Najet drilling (North American Aviation Inc., process) uses a flat-tipped bit with controlled torque and pressure to prevent damaging the bit. The bits are made to an L/D value of 7. It was possible with this equipment to drill holes as small as 0.009 inch in diameter at an angle of 30 degrees to the axis of the nickel tube and 0.008 inch at an angle of 25 degrees to the axis of the CRES tube. Using an electrodischarge machining technique (process of removing metal with electric arc), holes 0.008 inch in diameter were placed in the nickel tubing at an angle of 10 degrees to the tube axis.

4. BRAZING

(U) Brazing was used extensively in assembling the hot-firing segments and the honeycomb structural segment. The braze alloys used are described in Table 3. Good bonds were achieved in these components by maintaining high cleanliness standards and assuring proper bonding pressure during brazing. The important details of the various braze operations are presented in the following paragraphs.

a. Copper Brazing

(U) The solid-wall combustion chamber sections which were not of unit construction and the tube-wall throat insert core pieces were brazed as follows. The four pieces, two contour walls and two side walls, were vapor degreased and cleaned just prior to assembly for brazing. The pieces were assembled in a clean room using wrinkle-free sheets of 0.002-inch thick 50-50 braze alloy. The assembly was placed in the furnace retort on a plate which was flat to 0.003 inch and weighted with 10 to 15 pounds of copper. Refrasil cloth was used to separate the assembly from the support plate and weights. The cloth had been prefired with dry hydrogen. The retort was purged with argon prior to heating and while the assembly was slowly heated to 1400 F. From 1400 F to the braze temperature, the argon was replaced with a hydrogen purge. The assembly was held at the 1800 F braze temperature for 10 minutes then slowly cooled. Thermocouples in the assembly were monitored to maintain minimum thermal gradients while heating and cooling. Argon was resubstituted for hydrogen below the 1400 F temperature.

(U) The core to collar assemblies of the solid wall segments were brazed using a eutectic bonding method. The outside diameter of the core was plated with 0.0015 inch of silver and the inside diameter of the collar machined to produce a 0.002 inch shrink fit. The shrink fit was obtained by chilling the core and heating the collar immediately prior to assembly. The core was sealed in an airtight container to prevent oxidation after plating and prior to assembly. The collar was vapor degreased and cleaned prior to assembly. The braze cycle was similar to that used to join the walls of the core together except that the braze temperature was approximately 1500 F.

(U) Brazing the tubes to the support structures for the tube-wall throat insert and the tube wall segments was accomplished using Nicoro alloy. The tubes were weighted during the braze cycle to achieve close contact with the backup structure. The weight was again separated from the tubes by a thin layer of refrasil cloth to prevent diffusion bonding.

b. <u>Inconel 718 Brazing</u>

(U) A critical area in the honeycomb panel design for the structural segment is that of the braze bonds between the core sections and the face sheets. These bonds must transmit shear loads equal to those taken by the core. Once a particular cell size and consequent bond length per unit face sheet area is chosen, bond strength is a function of braze alloy shear strength and size of the fillets formed by the alloy. Figure 32 presents fillet size requirements vs braze alloy shear strength. As the silver based alloys usually used for brazed honeycomb bonding have insufficient strength at MSPS operating temperatures, a higher melting point alloy, Palniro 7 (70 Au-8 Pd-22 Ni) was evaluated for the segment panels. This alloy has an ultimate shear strength of 26,000 lb/sq in. at 1200 F, the maximum structure temperature expected in the MSPS engine.

(U) <u>Subscale Samples</u>. Two subscale braze samples were prepared to check aspects of the planned honeycomb panel assembly braze cycle. In particular, the stack pressure, alloy fillet size, wetting properties, and aggressive characteristics were of interest. Both full and subscale panel samples were brazed in an inner retort box. The five sided box was welded together from 0.250 inch-thick Inconel 600 plate. The honeycomb sandwich assemblies were placed inside the box and a thin sheet of metal foil was welded over the top of the retort. By partially evacuating the retort, any pressure up to a full atmosphere could be applied through the foil to the honeycomb sandwich assembly. Adequate pressure must be applied to insure contact between the core and the braze alloy foil tack welded to the face sheets, while excessive pressure would crush the core. The pressure used was scaled from that used during lower temperature honeycomb brazing at Los Angeles Division of North American Aviation Inc. To insure that air would not leak into the inert argon atmosphere in the inner retort, an outer retort was placed around the inner and filled with additional argon at atmospheric pressure.

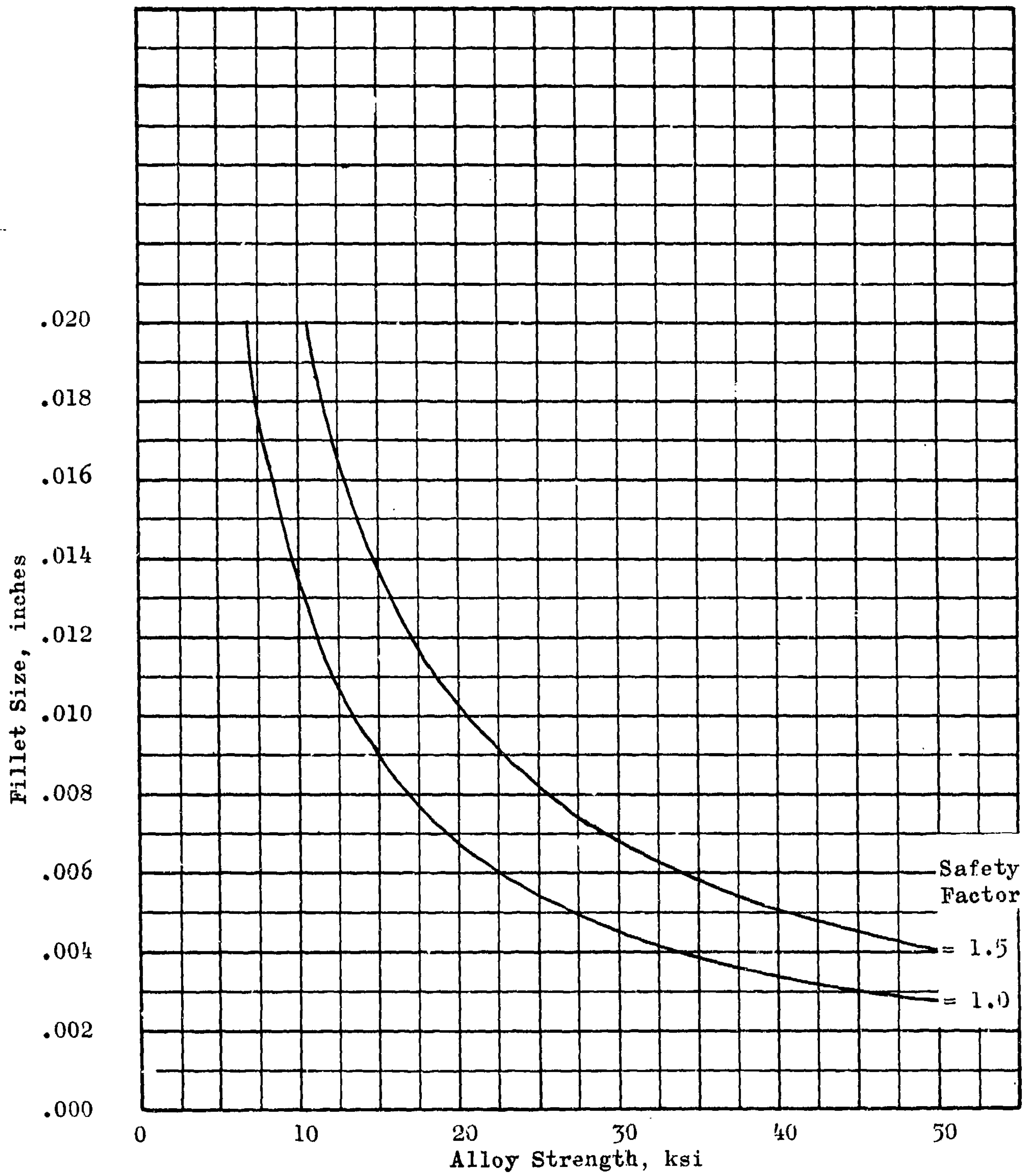

Figure 32 . Required Fillet Size vs Alloy Strength

(U) One of the subscale braze samples employed Palniro No. 7 alloy with a thin plating of nickel on the braze surfaces, the other used the same alloy without plating. As no trouble with wetting, fillet size or erosion of the thin gage core foil was found in either of the two subscale samples, no specimens were brazed with alternate alloys. The thin nickel plating over the brazed surfaces did produce slightly better wetting of the surface, and was used on the full scale panel sample. Fillet sizes measured on microsections of samples brazed with Palniro 7 were between 0.006 and 0.007 inch. The bonds are thus adequate for the structural test segment. Figure 33 is a microphoto of the joint.

(U) Full Scale Panels. A full size honeycomb panel was brazed next. This sample was intended to verify design factors that could not be checked at the subscale level, e.g., whether the tooling to be used for the segment panels was adequate to ensure braze bonds at all necessary points in the assembly. The panel assembly, consisting of inner and outer face sheets, forward and aft core sections, and an intercore splice sheet, was sandwiched between relatively thick upper and lower form blocks of Inconel 718 cut to the desired shape of the final panel as shown in Fig. 14. A system of holes and grooves were machined into the form blocks to permit replacement of air and inert argon throughout the perforated core cells.

(U) Diffusion bonding between form blocks and face sheets was prevented by placing stopoff coated parting sheets of 0.010 thick CRES foil between them. Temperature and thermal gradients were monitored by three thermocouples. The first was placed at the periphery of the assembly, the other two through machined ports to the centers of the upper and lower form blocks, respectively. Pressure was applied to the sandwich by partially evacuating the inner retort as with subscale samples.

(U) Ultrasonic inspection of the panel indicated good braze joints at all locations except the miter joint between the fore and aft core pieces. This occurred because the radius of curvature of the bend on the face sheets was too large. The sheets were bent more sharply for the final panels and good bonding over the entire surface resulted.

5. WELDING

(U) Welding was used extensively in two areas of fabrication in this program: formation of tube bundles and fabrication of the structural segments. In all cases electron-beam welding was used to provide lightweight welds.

a. Coolant-Tube Bundle

(C) For the tube-wall segment, a novel method of bonding the tubes to each other and forming them to the desired contour was employed. Instead of forming each tube individually and brazing them to each other and to the support structure, the tubes were electron beam welded together to form a continuous flat tube bundle and then formed to the shape of the contour as shown in the sample tube bundle depicted in Fig. 34. This

Figure 33. Face Sheet to Honeycomb Braze

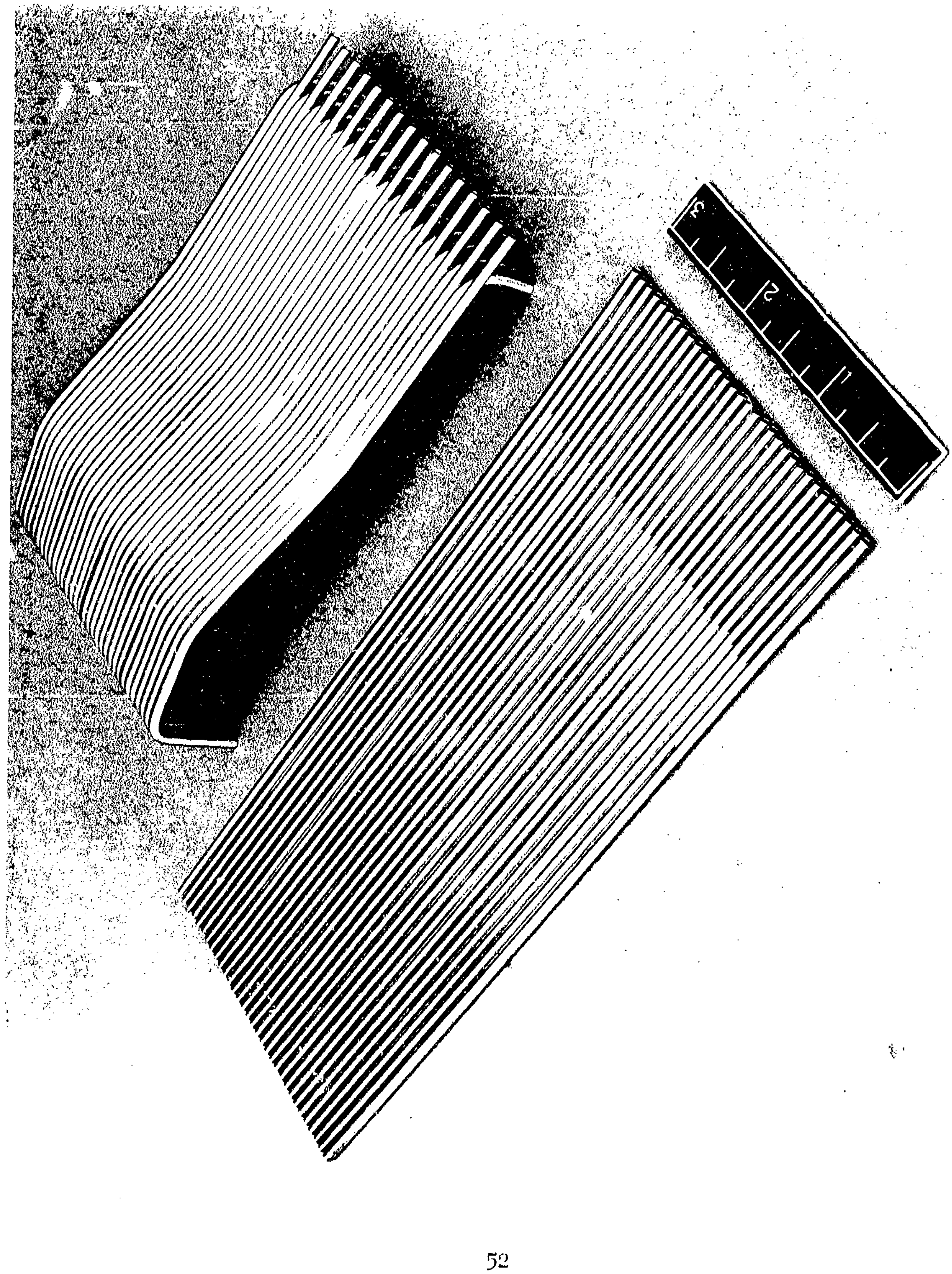

Figure 34. Sample EB-Welded Tube Blankets
Before and After Forming

(C) assembly technique results in a more uniform tube bundle cross section, eliminates the possibility of braze washout between tubes, facilitates controlling the tube cross section during the forming operation, and decreases the effort required to form and braze tubes to the strongback. A microphoto of electron beam welded nickel tubes is shown in Fig. 35. The excellent bond formed by the parent material of the tubes is apparent. A lightweight joint is formed because no additional weld material is used in the process. After determining the required equipment settings on the basis of a sample run, the welder can be operated at a maximum speed of 50 inches per minute. The width of the weld and depth of penetration can be controlled over wide ranges. The welding is accomplished under vacuum conditions in a shielded chamber the dimensions of which establish the limits of the size of the component to be welded. Figure 36 is a cross section of an electron beam welded CRES 347 tube bundle. A 100X microphoto of the weld is also shown in Fig. 36.

(C) The tubes were welded together in the flat form. To keep the stack flat, the tubes were held in a fixture which clamps the tube ends against a flat plate. To prevent accumulation of weld shrinkage, every other joint was skipped on the first weld sequence resulting in groups of two tubes welded together. This distributed the weld shrinkage evenly over the remaining joints. The process was repeated, welding the groups of two into groups of four, etc., until the entire stack was welded together. The beam was started and stopped off of the tube blanket to prevent burning holes in the tubes during electronic transients. The unwelded end portions of the stacks which were under the fixture clamps were subsequently trimmed off. The stacks were then bent much like a piece of sheet metal to match the chamber contour.

b. <u>Rib Structural Segment</u>

The panels of the rib structural segment shown in Fig. 11 consisted of U-shaped channels which formed the inner combustion chamber contour and provided rigidity to the segment. During assembly, these channels were stacked in closeout plates. The plates were then rigidly held in a fixture during welding to keep the panel straight and hold the distance between ends. The channels were first welded to each other and then to the closeouts. The channels and closeouts for one panel are shown in Fig. 37.

(U) <u>Weld Samples</u>. Prior to starting the actual fabrication, a brief sampling program was conducted to determine whether Tungsten Inert Gas, TIG, or Electron-Beam, E-B, welding would be used to assemble the panels. TIG welding has the advantage of requiring less exact fitting tolerances prior to welding since the weld rod metal can bridge small surface discontinuities. However, if proper fitting tolerances can be held, the EB welding technique results in a cleaner weld. The EB welding process also results in less weld shrinkage than TIG welding. The width and penetration depth of the weld are determined by control settings on the equipment. Once these proper settings have been determined by a sample weld, all channel welds are made at the same settings so that a uniform weld is rapidly made. Test samples of

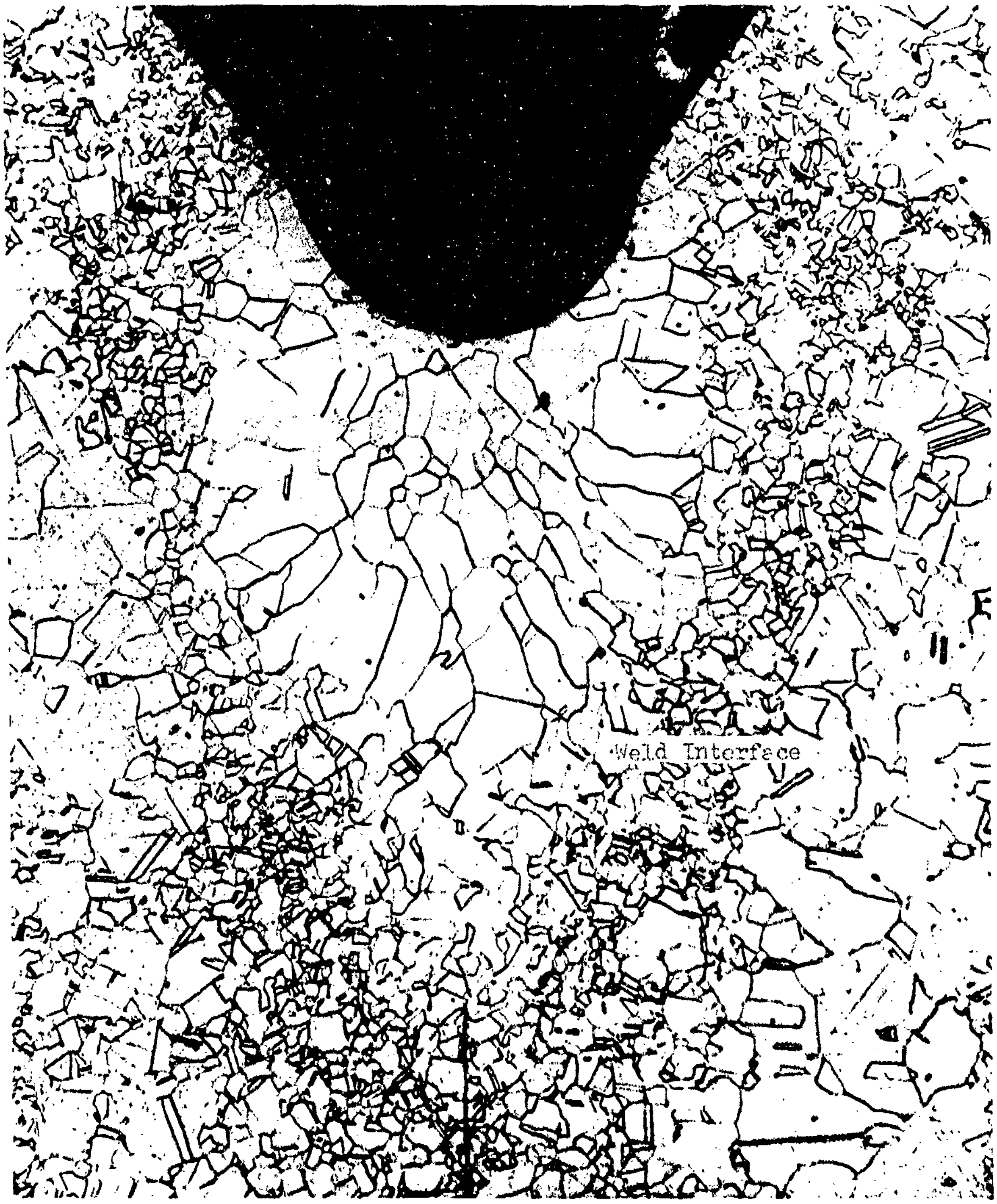

Figure 35. Microphoto of Electron-Beam Welded Nickel Tubes

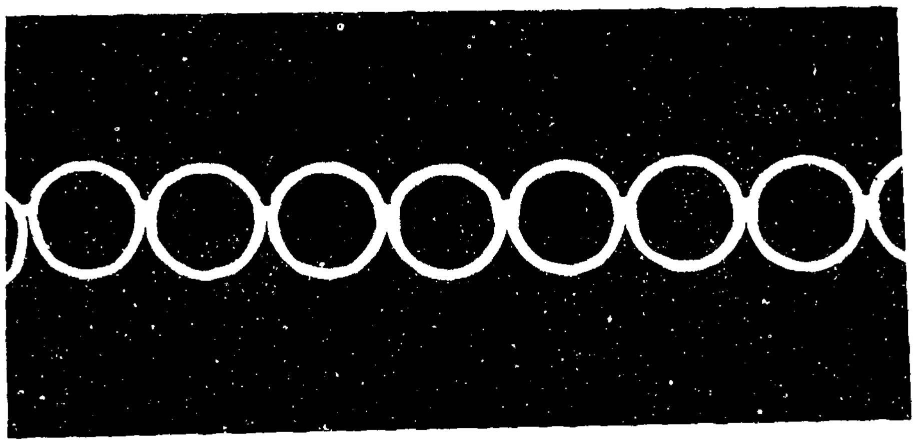

MAG. 6X Etchant: $HCl:H_2O_2$

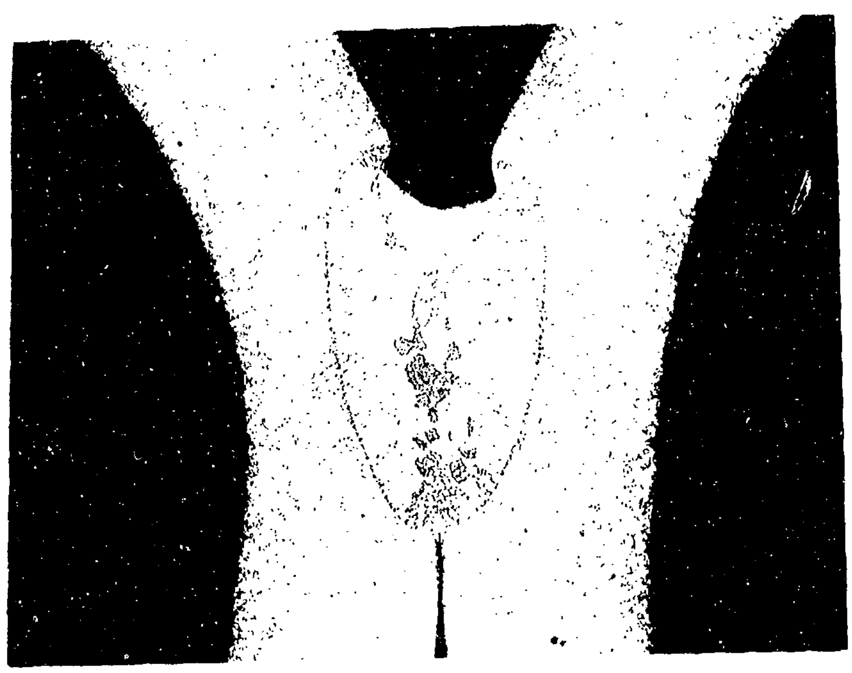

MAG. 100X Etchant: $HCl:H_2O_2$

Figure 36. Electron Beam Welded CRES 347 Tubes

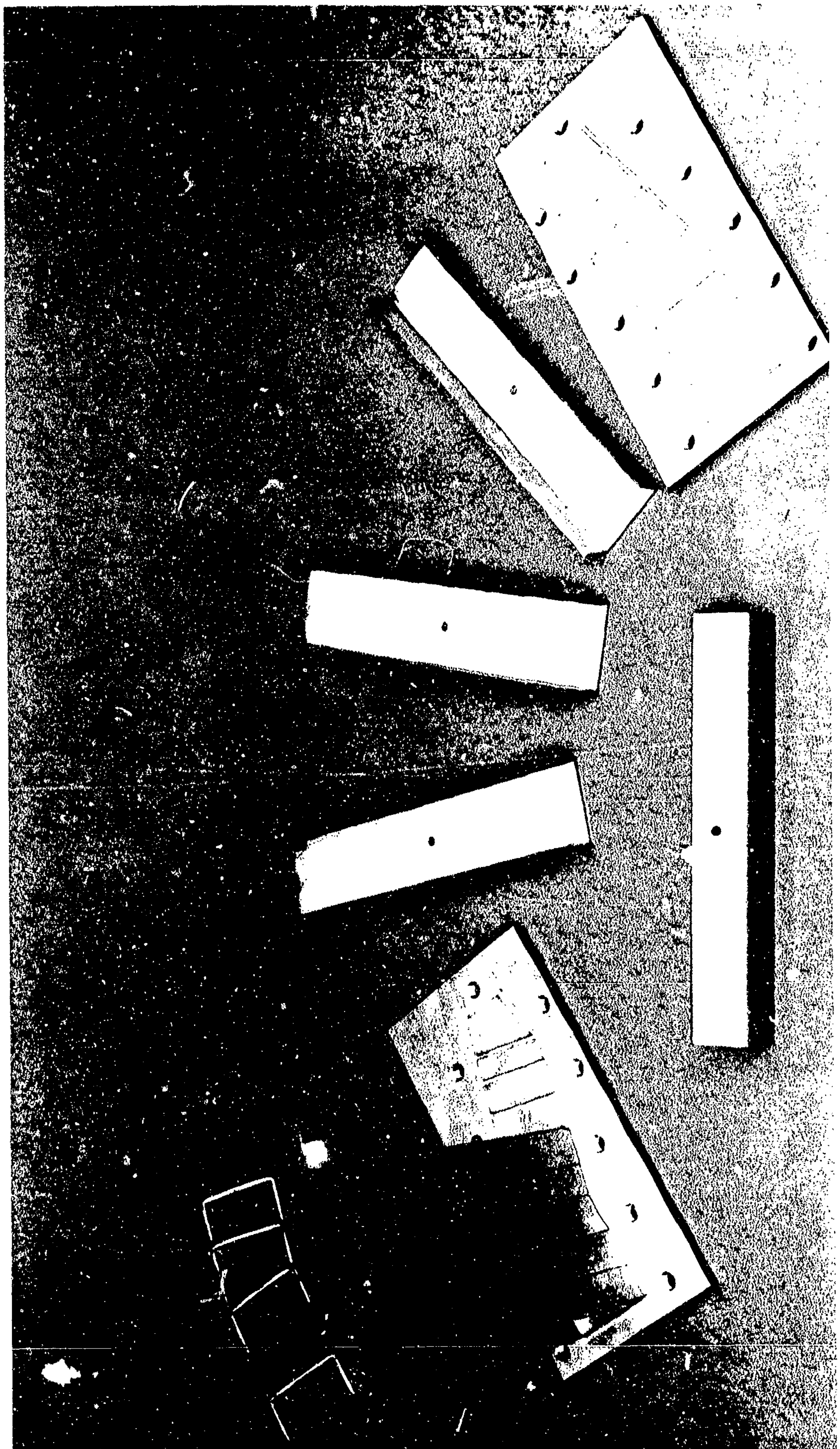

Figure 37 . Partial Assembly of Rib Panel

(U) channels were EB welded to provide the optimum equipment settings and to determine if fitup problems did exist. The fitup design and techniques proved to be quite compatible with the EB welding process, and very good samples were obtained.

(U) The EB weld joints on a three-channel sample are shown in Fig. 38. These channel-to-channel welds indicated good uniformity and penetration as shown by the microphotos. The strength of these welds is presented later in the heat treatment discussion. The channel-to-closeout welds on the sample are shown in the microphotos in Fig. 39. The top photo of the weld between the center portion of the channel end and the closeout is especially interesting because of its good positioning in a completely "blind" location. On the basis of these samples the EB welding process was used to assemble the channels and closeouts. The same process was used for the assembly of the other components of the segments, i.e., welding the side plates and baffles to the injectors and welding the panels to the injectors and baffles.

(C) Final Panel Assembly. The pieces for the assembly of one panel were shown in Fig. 37. Five "U" channels are shown stacked on one of the closeout plates. The grooves in the closeouts index the channels to minimize distortion during welding. The "U" channels were formed from 0.044-inch sheet stock by a punch and die. They were then match machined to the indexing grooves in the closeout plates. The raised portion in the center of the closeout plate matches the inside and outside chamber contours and is the only part of the plate that remains after the panel is trimmed on the ends to fit between the chamber baffles. Figure 40 shows the fitted panel assembled in the weld fixture before weld. The fixture was used to maintain alignment between closeout plates thus minimizing warpage during welding. The fixture was made of annealed Inconel 718 plate so that it could be used to anneal the panel assembly, however, annealing was not necessary because the distortion during welding was negligible.

(C) The first step in the welding process was to weld the sheet metal "U" channels to each other. The legs of the channels were first tack welded to the adjoining channel to prevent separation during electron beam welding. The legs of each channel were then electron beam welded to the chamfered radius of the adjoining channel. To compensate for the slightly greater tolerances in the full-length channels compared to the samples, the electron beam weld between channels was made using two passes with the beam oriented perpendicular to the chamber wall portion of the channels. After the channels were welded to each other, the sides of the ends of the channels were butt welded to the closeouts. The web portion of the channels was then attached to the closeouts by welding through the closeout into the web. A completed panel except for finish machining of closeouts is shown in Fig. 41.

(U) The finished structural panels were inspected by dye penetrant and ultrasonic scan. The first panel was also X-rayed. The dye penetrant was used to detect surface cracks in the welds. There were a few small indications which were rewelded before final assembly. The first panel was both X-rayed and ultrasonic inspected to determine the quality of

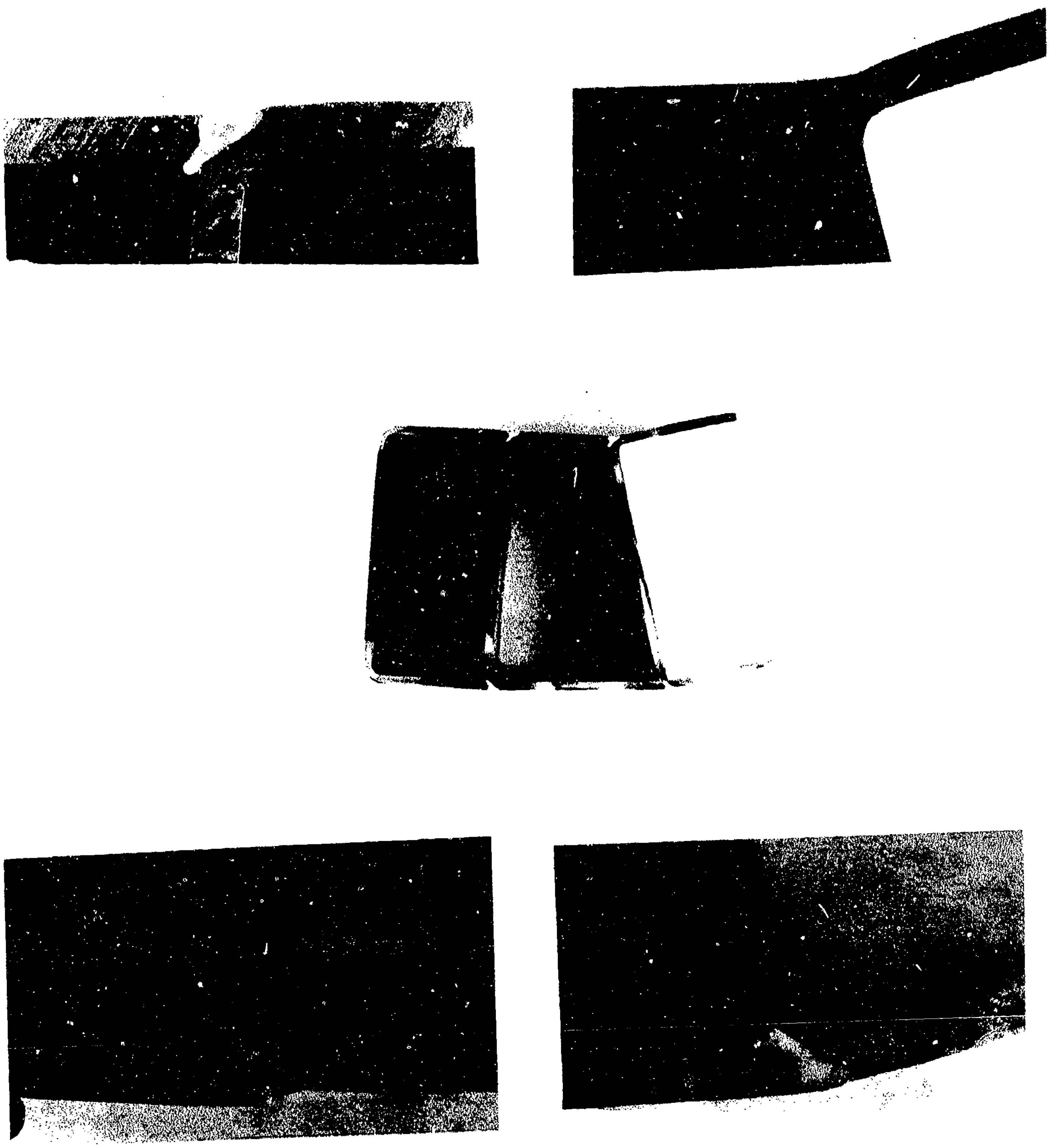

Figure 38. Rib Weld Sample

Channel End to Closeout Blind "Tee"

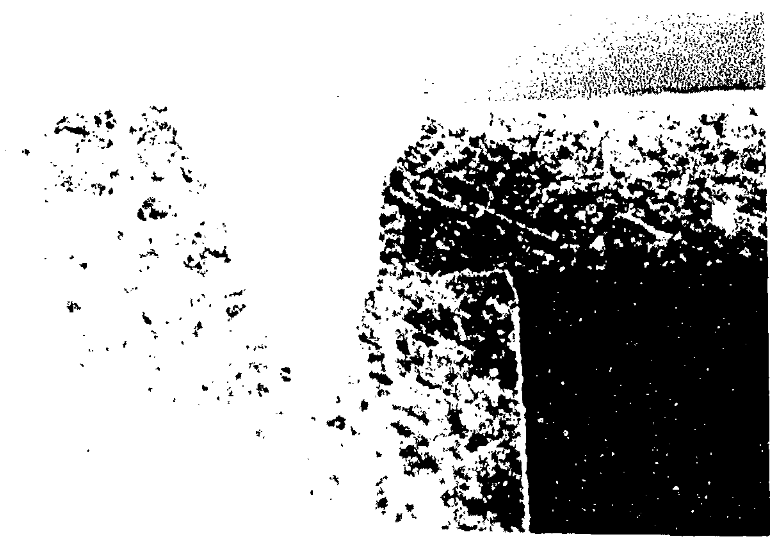

Channel End Side to Closeout Butt Weld

Figure 39. Final Weld Configurations Selected for Welding Channel Ends to Rib Section Closeouts.

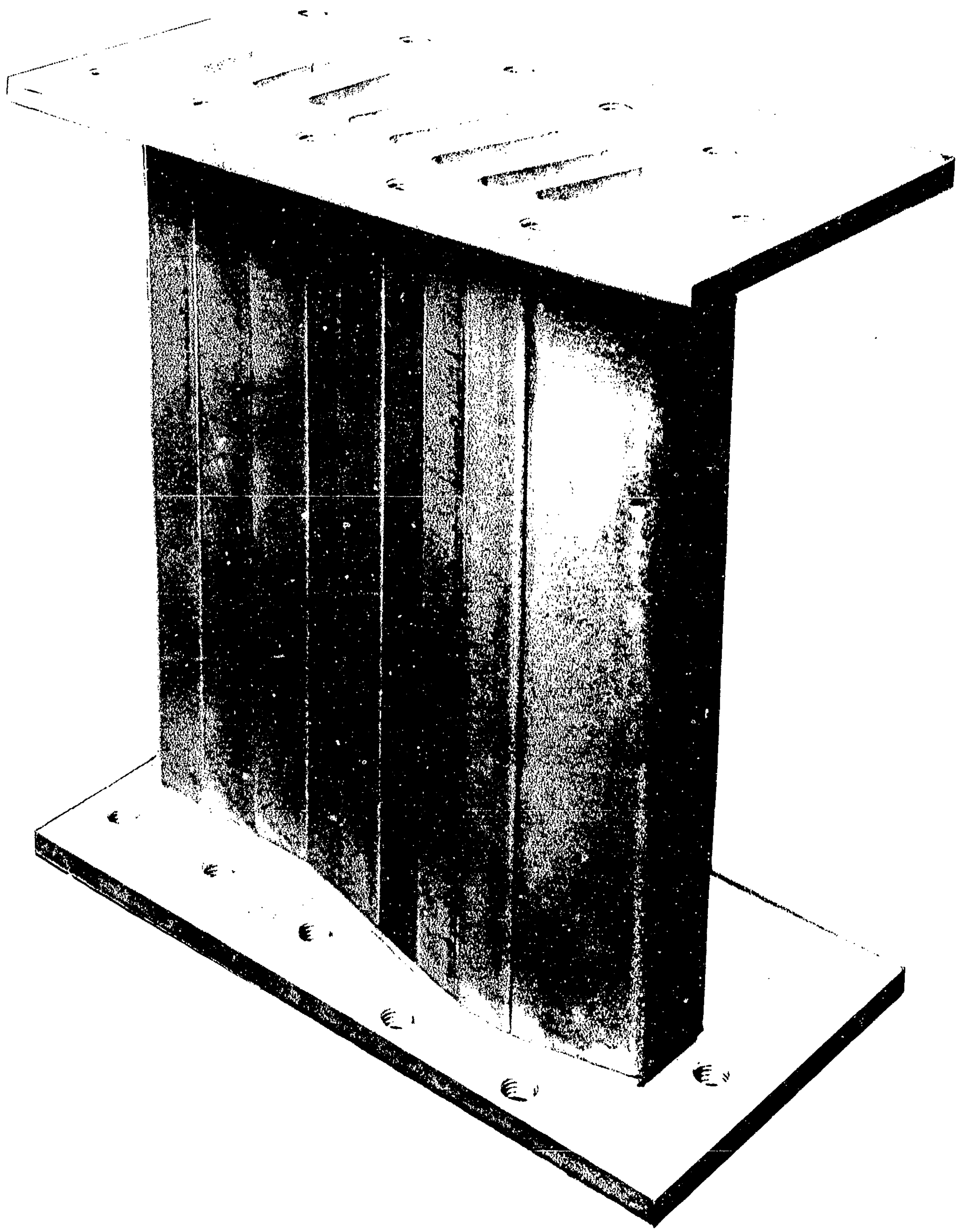

Figure 40. Rib Panel Before Welding

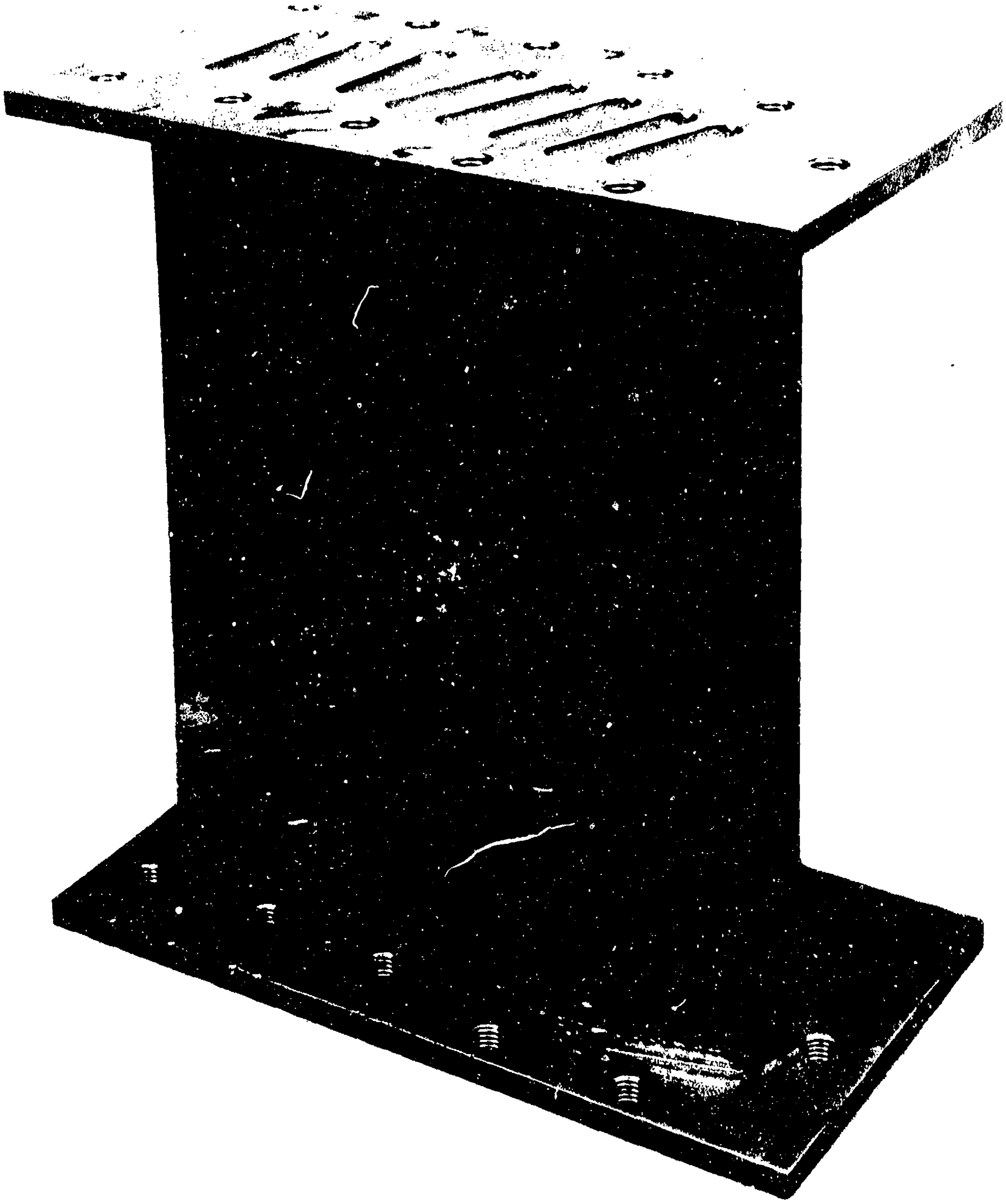

Figure 41. Rib Panel After EB Welding

(U) the web to closeout welds which were blind joints. The X-ray pictures were not very informative because it was not possible to shoot across the joint. The ultrasonic inspection was done on the ends of the panel to determine if structural continuity existed between the panel webs and the closeout. This type of inspection was successful. The joint area and some small unbonded areas were indicated. The indicated unwelded areas were not large enough to require reweld. It was not practical to section one of the panels to verify the validity of the ultrasonic tests but it appears to be an acceptable inspection technique for the web to closeout weld.

c. Honeycomb Structural Segment

(U) The honeycomb core sections resist shear loads on the panel. These shear loads are transmitted to the baffles through an electron beam weld between the nickel plated core and the baffle. The face sheets transmit the forces arising from the bending moments to the baffles. The shear stress was sufficiently low that degradation of the Inconel 718 strength by nickel diffusion was inconsequential as determined by the weld sample described below. However, the face sheets were highly stressed so that a 0.060-inch thick Inconel 718 closeout was placed between the electroformed nickel and the baffle. The nickel layer was first electron beam welded to the honeycomb panel closeout to transmit shear, then the face sheets were brazed over this joint. Finally an electron beam weld was made joining closeout and face sheet to baffle. An intermediate closeout was not necessary at the more lightly loaded honeycomb panel to injector weld.

(U) The nickel plated block used for the plating sample evaluation was incorporated into a mechanical test specimen designed to establish the shear strength of the electron beam weld between Inconel 718 and the plated nickel layer (Fig. 42). The nickel plated Inconel 718 inner block was welded between the arms of a U-shaped outer block, also of Inconel 718. The loading of this sample would simulate the shear loading in the actual segment due to chamber pressure as illustrated in Fig. 43.

(U) Four welds were made between the plating layer and the U-shaped block, along top and bottom of the two opposite flat sides of the rectangular block. Weld penetration was sized so that the specimen would fail in shear across the welds unless the adhesion of the plating layer to the inner block was much weaker than expected. As the weld beads were essentially castings of molten Inconel 718 plus pure nickel, it was expected that the weld shear strength would be intermediate between that of pure annealed nickel and that of Inconel 718, a nickel base alloy.

(U) The specimen was heat treated after weld in a cycle that produced both the high annealing temperature expected during the honeycomb panel braze cycle (1950 F) and the age hardening (8 hours at 1325 F) to be used during the panel attachment weld heat treat. Thus any unfavorable metallurgical reactions to occur in the segment would have been duplicated in the weld sample.

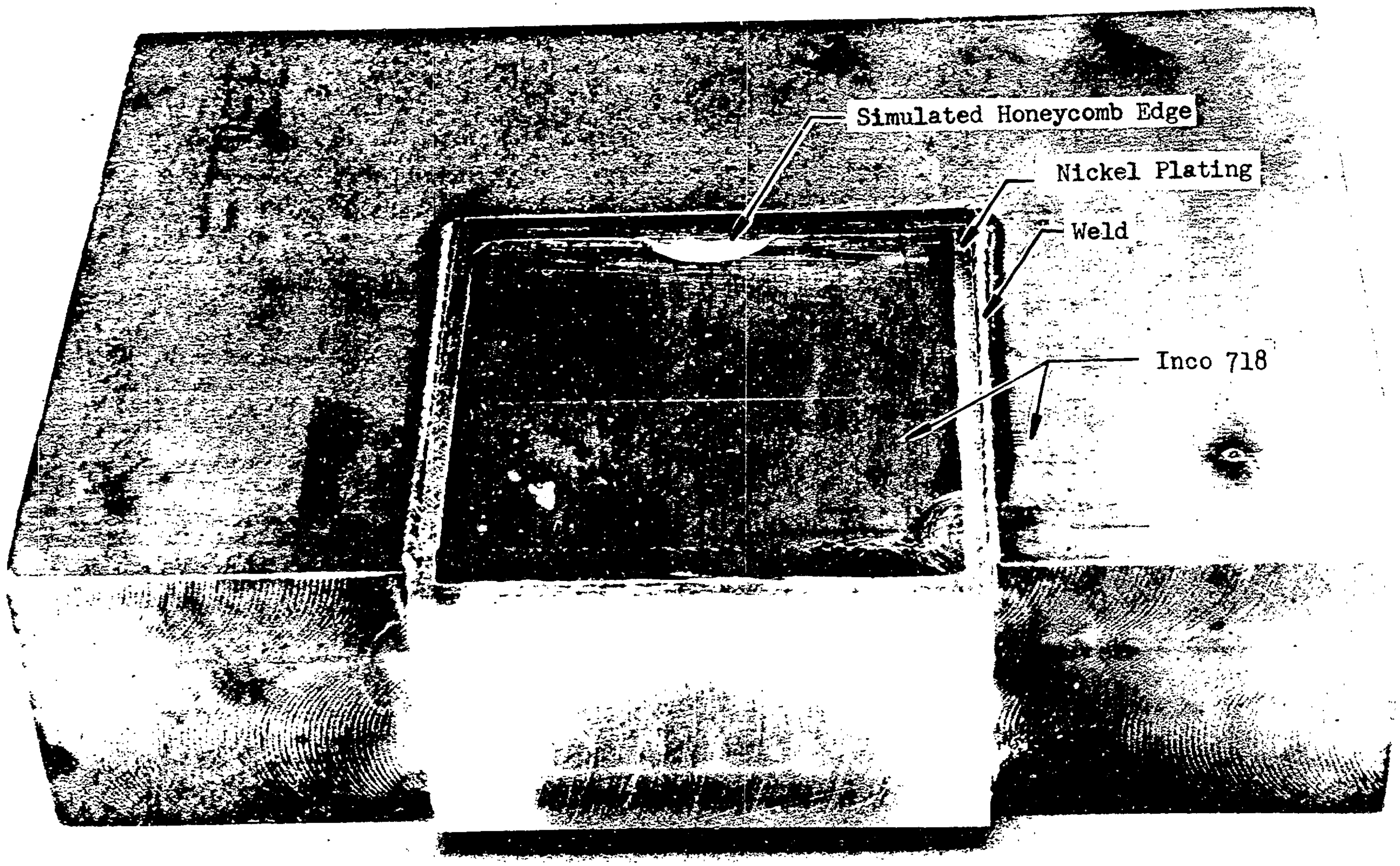

Figure 42. Nickel Plating and Weld Sample

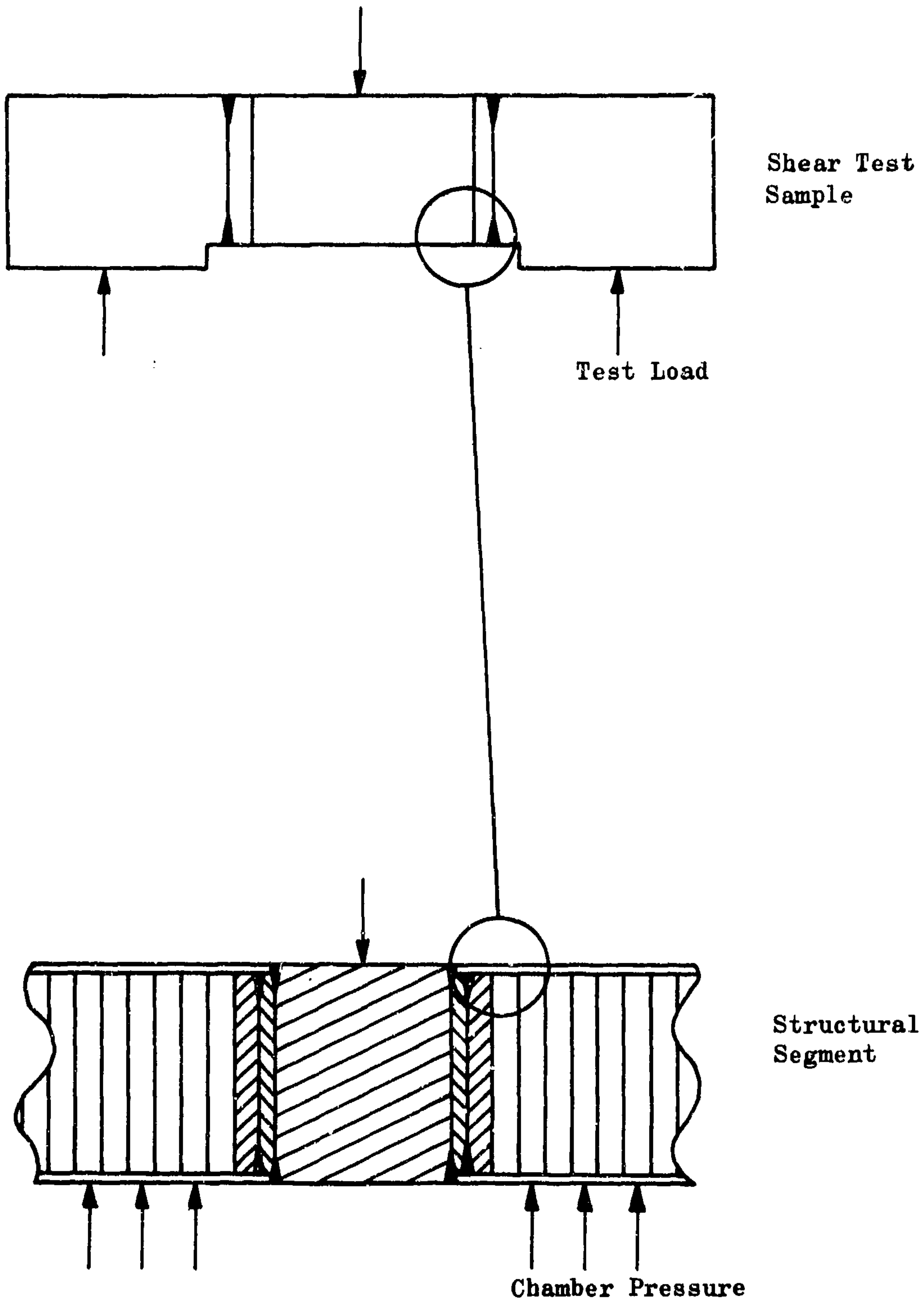

Figure 43. Plated Edge Joint Weld Sample

(U) Before mechanical testing, a thin slice through the weld cross sections of the specimen was removed for etching and microphotography. Microscopic and fluorescent dye penetrant inspection of this section indicated that the electron beam was misaligned on one of the four welds, producing incomplete fusion and penetration. As a result, a wider beam was used on the segment welds.

(U) The specimen was tested to failure between the plattens of a compression testing machine. Inspection of the parted sample indicated that diffusion bonding had occurred over part of the area between unwelded portions of the two blocks during heat treat. This bonded area and the incomplete penetration of the fourth weld were compensated for in the calculation of weld failure stress. The resulting ultimate shear strength was 40,000 psi, i.e., double the strength of nickel plating or one-fourth the strength of Inconel 718. The plating layer exhibited excellent ductility and adhesion to the inner block. Thus, the weld specimen test showed that the structural panel to baffle shear joint design was entirely adequate under the calculated load.

6. HEAT TREATING

(U) Both the rib and the honeycomb structural segments were heat treated after the weld assembly was completed to develop the strength of the Inconel 718 and to relieve stresses incurred during the welding operation. This heat treatment consisted of raising the temperature slowly to 1775 F; holding this temperature for 25 minutes; cooling to 1325 F and holding for 8 hours; cooling to 1150 F and holding for 8 hours; cooling to room temperature.

(U) Samples of the electron beam welded rib structure were subjected to this heat treatment. The resulting specimens were structurally tested together with weld samples that were not heat treated and samples of the as received Inconel 718. The results of these tests and an etched microphotograph of a heat treated sample are presented in Fig. 44.

Test Conditions	UTS	YTS .2% Offset	Elongation in 1/2 in.	
As Received - Longitudinal	114.7	51.7	70.0	
- Transverse	115.6	50.2	66.0	
As Welded	93.3	——	——	④
Unwelded Material After Heat Treat ①②				
- Transverse	174.7	113.8	16.0	④
- Longitudinal	179.3	118.3	16.0	④
Weld Joint After Heat Treat ①③	130.9	112.0	6.0	④

① Heat treat 1775°F - 25 minutes + 1325°F - 8 hours + 1150°F - 8 hours

② Standard Tensile Bars

③ Modified Tensile Bar As Shown

④ Average of 3

Figure 44. Typical Channel to Channel Rib Panel Weld

SECTION V

CONCLUSIONS AND RECOMMENDATIONS

(C) As a result of the experience gained with the processes described in Section IV, the following may be concluded:

1. An improved braze bond between honeycomb core and face sheets can be obtained by flash plating the core with nickel prior to brazing.
2. Further refinements of the plating process used are required to produce a copper coated CRES coolant tube suitable for brazing.
3. An excellent nickel coating can be electroformed onto a tapered nickel tube. However, for small diameter tubes the subsequent grinding process must be improved to obtain a concentric constant O. D.-variable I. D. tube.
4. Electroforming the edges of honeycomb with nickel is a satisfactory method of preparing the honeycomb for welding to a thick member.
5. Palniro No. 7 is a satisfactory alloy for brazing honeycomb to face sheets for high temperature applications.
6. Electron beam welding of coolant tubes prior to forming provides an efficient method of producing a tube bank.

(C) A comparison of the results of the coolant tube electroforming process indicates that nickel on nickel forming is more advanced than copper on CRES forming. It is recommended that the nickel tubes be used in applications requiring tubes of sufficiently large diameter to obviate difficulties in grinding after electroforming. Methods of improving the grinding process after plating should be investigated for small tubes.

(C) The use of electron beam welded tube bundles is recommended where applicable to eliminate the necessity of forming individual tubes and provide a uniform tube bundle surface.

(U) The fabrication of samples is highly recommended for processes where novel techniques or materials are required. This procedure is particularly economical when only a small number of end items are required. Careful planning of the sample program is necessary to assure that the sample has the essentials of the end item while maintaining as low a complexity level as possible.